anti-dystrophin (NCL-DYS1, 1:10, and NCL-DYS2, 1:50, Novocastra), anti-spectrin (MAB1622, Clone AA6, 1:200, Millipore, Schwalbach, Germany), anti-α-sarcoglycan (NCL-a-SARC, 1:50, Novocastra) and anti-β-dystroglycan (NCL-b-DG, 1:10, Novocastra). The isotype-specific secondary antibodies were anti-mouse IgG (H+L) coupled to Alexa Fluor 488 (A11029, 1:300, Invitrogen) and anti-mouse IgG coupled to TRITC (R0270, 1:300, Dako, Glostrup, Denmark). Utrophin immunohistochemistry was performed on sections of formalin-fixed and paraffin-embedded samples of the biceps femoris muscle of each two 2-day-old and 3-month-old DMD pigs and age-matched WT controls, using a polyclonal rabbit anti-utrophin antibody (sc15377, 1:100, Santa Cruz Inc., USA) according to the standard avidin–biotin peroxidase complex method (secondary antibody: biotinylated goat anti-rabbit immunoglobulins, E0432, Dako). Diaminobenzidine was used as the final chromogen and haemalum as nuclear counterstain. For negative controls, slides were incubated with an irrelevant primary antibody (polyclonal rabbit anti-*Escherichia coli*, B0357, Dako) instead of the anti-utrophin antibody.

Morphometric analyses

Morphometric analyses were performed on H&E-stained plastic (GMA/MMA) cross-sections of the left and right biceps femoris muscle of three 2-day-old and five 3-month-old DMD pigs, and of corresponding age-matched control pigs ($n = 3$ and 3, respectively). For quantification of muscle fibre sizes, at least 12 locations per case were taken by systematic random sampling in the sections at ×250 magnification, and superimposed with an unbiased counting frame (58). The minimal Feret's diameters of all muscle fibre cross-section profiles ($n = 697 \pm 166$) sampled with the unbiased counting frames were measured (59), using a Videoplan image analysis system (Zeiss-Kontron, Munich, Germany). To display the distribution of fibre diameters, the percentage deviation of each single measured muscle fibre diameter from the mean diameter of all muscle fibres was calculated separately for each investigated case. The respective single values were categorized into 23 classes of 10% deviation of the mean fibre diameter. The number of single values per class was counted, and their respective proportion (%) of the total number of evaluated fibre diameters was calculated. The volume density of muscle fibres in the biceps femoris muscle was determined by point counting (60) (294 ± 0.6 points per case) in six systematically randomly sampled locations at ×250 magnification, using an automated stereology system (VIS-Visiopharm Integrator System® Version 3.4.1.0 with newCAST® software, Visiopharm A/S, Hørsholm, Denmark). In the same locations, the proportion of muscle fibre cross-section profiles displaying at least one internalized centrally located nuclear section profile was determined, using an unbiased counting frame. Per case, 723 ± 250 muscle fibre cross-section profiles were evaluated.

Data analysis

Data are presented as means ± standard deviations. Unpaired two-sided *t*-tests were used for statistical analysis, assuming equal variances for the parameter body weight, and unequal variances for morphometric muscle parameters. The correlation between birth weight and life expectancy was evaluated using GraphPad Prism. *P*-values of < 0.05 were considered statistically significant.

SUPPLEMENTARY MATERIAL

Supplementary Material is available at *HMG* online.

AUTHOR CONTRIBUTIONS

N.K., C.T., H.L., M.C.W. and E.W. designed the study. N.K., A.B., S.K., K.B., A.W., St.K., A.G., B.K., V.Z., M.K., E.K., H.N., B.S., N.H., H.B., R.W., M.C.W. and E.W. performed experiments and analysed data. N.K., H.L., M.C.W. and E.W. wrote the paper with contributions from all authors. N.K, A.W. and K.B. did the gene targeting experiments. B.K., V.Z., M.K. and H.N. were involved in nuclear transfer experiments. St.K., A.G. and H.B. performed the RNA expression and bioinformatics studies. S.K. and B.S. did the immunofluorescence, A.B. the immunohistochemistry and E.K. the western blot analyses. A.B., K.B., N.H. and R.W. performed the pathological and stereological studies. B.K., M.C.W. and E.W. designed the locomotion studies. A.A.-R. contributed to the discussion. H.L., M.C.W. and E.W. gave conceptual advice and supervised the project.

ACKNOWLEDGEMENTS

We thank Maria Schmuck, Ursula Klutzny, Tuna Güngör, Anne Richter, Heike Sperling, Lisa Pichl, Christian Erdle and Sigfried Elsner for excellent technical assistance. Further we thank Dr Simone Renner, Dr Andrea Bähr, Andrea Beck, Christina Braun-Reichhart and Elisabeth Streckel for expert veterinary care.

Conflict of Interest statement. None declared.

FUNDING

Grant support was obtained from the Bavarian Research Foundation (AZ 802/08), from Aktion Benni & Co. (German Duchenne Parents Foundation), from Sirion Biotech GmbH, Planegg, Germany, from MWM Biomodels GmbH, Tiefenbach, Germany, and from Minitüb GmbH, Tiefenbach, Germany.

REFERENCES

1. Hoffman, E.P., Brown, R.H. Jr and Kunkel, L.M. (1987) Dystrophin: the protein product of the Duchenne muscular dystrophy locus. *Cell*, **51**, 919–928.
2. Koenig, M., Beggs, A.H., Moyer, M., Scherpf, S., Heindrich, K., Bettecken, T., Meng, G., Muller, C.R., Lindlof, M., Kaariainen, H. *et al.* (1989) The molecular basis for Duchenne versus Becker muscular dystrophy: correlation of severity with type of deletion. *Am. J. Hum. Genet.*, **45**, 498–506.
3. Spurney, C.F. (2011) Cardiomyopathy of Duchenne muscular dystrophy: current understanding and future directions. *Muscle Nerve*, **44**, 8–19.
4. van Deutekom, J.C., Janson, A.A., Ginjaar, I.B., Frankhuizen, W.S., Aartsma-Rus, A., Bremmer-Bout, M., den Dunnen, J.T., Koop, K., van der Kooi, A.J., Goemans, N.M. *et al.* (2007) Local dystrophin restoration with antisense oligonucleotide PRO051. *N. Engl. J. Med.*, **357**, 2677–2686.
5. Aartsma-Rus, A., den Dunnen, J.T. and van Ommen, G.J. (2010) New insights in gene-derived therapy: the example of Duchenne muscular dystrophy. *Ann. N. Y. Acad. Sci.*, **1214**, 199–212.

6. Cirak, S., Arechavala-Gomeza, V., Guglieri, M., Feng, L., Torelli, S., Anthony, K., Abbs, S., Garralda, M.E., Bourke, J., Wells, D.J. *et al.* (2011) Exon skipping and dystrophin restoration in patients with Duchenne muscular dystrophy after systemic phosphorodiamidate morpholino oligomer treatment: an open-label, phase 2, dose-escalation study. *Lancet*, **378**, 595–605.
7. Fairclough, R.J., Wood, M.J. and Davies, K.E. (2013) Therapy for Duchenne muscular dystrophy: renewed optimism from genetic approaches. *Nat. Rev. Genet.*, **14**, 373–378.
8. Bulfield, G., Siller, W.G., Wight, P.A. and Moore, K.J. (1984) X chromosome-linked muscular dystrophy (mdx) in the mouse. *Proc. Natl. Acad. Sci. USA*, **81**, 1189–1192.
9. Im, W.B., Phelps, S.F., Copen, E.H., Adams, E.G., Slightom, J.L. and Chamberlain, J.S. (1996) Differential expression of dystrophin isoforms in strains of mdx mice with different mutations. *Hum. Mol. Genet.*, **5**, 1149–1153.
10. Araki, E., Nakamura, K., Nakao, K., Kameya, S., Kobayashi, O., Nonaka, I., Kobayashi, T. and Katsuki, M. (1997) Targeted disruption of exon 52 in the mouse dystrophin gene induced muscle Degeneration similar to that observed in Duchenne muscular dystrophy. *Biochem. Biophys. Res. Commun.*, **238**, 492–497.
11. Sharp, N.J., Kornegay, J.N., Van Camp, S.D., Herbstreith, M.H., Secore, S.L., Kettle, S., Hung, W.Y., Constantinou, C.D., Dykstra, M.J., Roses, A.D. *et al.* (1992) An error in dystrophin mRNA processing in golden retriever muscular dystrophy, an animal homologue of Duchenne muscular dystrophy. *Genomics*, **13**, 115–121.
12. Nakamura, A. and Takeda, S. (2011) Mammalian models of Duchenne Muscular Dystrophy: pathological characteristics and therapeutic applications. *J. Biomed. Biotechnol.*, **2011**, 184393.
13. Aigner, B., Renner, S., Kessler, B., Klymiuk, N., Kurome, M., Wunsch, A. and Wolf, E. (2010) Transgenic pigs as models for translational biomedical research. *J. Mol. Med. (Berl.)*, **88**, 653–664.
14. Rogers, C.S., Stoltz, D.A., Meyerholz, D.K., Ostedgaard, L.S., Rokhlina, T., Taft, P.J., Rogan, M.P., Pezzulo, A.A., Karp, P.H., Itani, O.A. *et al.* (2008) Disruption of the CFTR gene produces a model of cystic fibrosis in newborn pigs. *Science*, **321**, 1837–1841.
15. Muntoni, F., Torelli, S. and Ferlini, A. (2003) Dystrophin and mutations: one gene, several proteins, multiple phenotypes. *Lancet Neurol.*, **2**, 731–740.
16. Copeland, N.G., Jenkins, N.A. and Court, D.L. (2001) Recombineering: a powerful new tool for mouse functional genomics. *Nat. Rev. Genet.*, **2**, 769–779.
17. Kerr, T.P., Sewry, C.A., Robb, S.A. and Roberts, R.G. (2001) Long mutant dystrophins and variable phenotypes: evasion of nonsense-mediated decay? *Hum. Genet.*, **109**, 402–407.
18. Ervasti, J.M. (2007) Dystrophin, its interactions with other proteins, and implications for muscular dystrophy. *Biochim. Biophys. Acta*, **1772**, 108–117.
19. Estrada, J., Sommer, J., Collins, B., Mir, B., Martin, A., York, A., Petters, R.M. and Piedrahita, J.A. (2007) Swine generated by somatic cell nuclear transfer have increased incidence of intrauterine growth restriction (IUGR). *Cloning Stem Cells*, **9**, 229–236.
20. Blake, D.J., Weir, A., Newey, S.E. and Davies, K.E. (2002) Function and genetics of dystrophin and dystrophin-related proteins in muscle. *Physiol. Rev.*, **82**, 291–329.
21. Huang da, W., Sherman, B.T. and Lempicki, R.A. (2009) Systematic and integrative analysis of large gene lists using DAVID bioinformatics resources. *Nat. Protoc.*, **4**, 44–57.
22. Huang da, W., Sherman, B.T. and Lempicki, R.A. (2009) Bioinformatics enrichment tools: paths toward the comprehensive functional analysis of large gene lists. *Nucleic Acids Res.*, **37**, 1–13.
23. Supek, F., Bosnjak, M., Skunca, N. and Smuc, T. (2011) REVIGO summarizes and visualizes long lists of gene ontology terms. *PLoS ONE*, **6**, e21800.
24. Smoot, M.E., Ono, K., Ruscheinski, J., Wang, P.L. and Ideker, T. (2011) Cytoscape 2.8: new features for data integration and network visualization. *Bioinformatics*, **27**, 431–432.
25. Pescatori, M., Broccolini, A., Minetti, C., Bertini, E., Bruno, C., D'Amico, A., Bernardini, C., Mirabella, M., Silvestri, G., Giglio, V. *et al.* (2007) Gene expression profiling in the early phases of DMD: a constant molecular signature characterizes DMD muscle from early postnatal life throughout disease progression. *FASEB J.*, **21**, 1210–1226.
26. Haslett, J.N., Sanoudou, D., Kho, A.T., Han, M., Bennett, R.R., Kohane, I.S., Beggs, A.H. and Kunkel, L.M. (2003) Gene expression profiling of Duchenne muscular dystrophy skeletal muscle. *Neurogenetics*, **4**, 163–171.
27. Porter, J.D., Merriam, A.P., Leahy, P., Gong, B. and Khanna, S. (2003) Dissection of temporal gene expression signatures of affected and spared muscle groups in dystrophin-deficient (mdx) mice. *Hum. Mol. Genet.*, **12**, 1813–1821.
28. Subramanian, A., Tamayo, P., Mootha, V.K., Mukherjee, S., Ebert, B.L., Gillette, M.A., Paulovich, A., Pomeroy, S.L., Golub, T.R., Lander, E.S. *et al.* (2005) Gene set enrichment analysis: a knowledge-based approach for interpreting genome-wide expression profiles. *Proc. Natl. Acad. Sci. USA*, **102**, 15545–15550.
29. Catoire, M., Mensink, M., Boekschoten, M.V., Hangelbroek, R., Muller, M., Schrauwen, P. and Kersten, S. (2012) Pronounced effects of acute endurance exercise on gene expression in resting and exercising human skeletal muscle. *PLoS ONE*, **7**, e51066.
30. Warren, G.L., Summan, M., Gao, X., Chapman, R., Hulderman, T. and Simeonova, P.P. (2007) Mechanisms of skeletal muscle injury and repair revealed by gene expression studies in mouse models. *J. Physiol.*, **582**, 825–841.
31. Valenzuela, D.M., Murphy, A.J., Frendewey, D., Gale, N.W., Economides, A.N., Auerbach, W., Poueymirou, W.T., Adams, N.C., Rojas, J., Yasenchak, J. *et al.* (2003) High-throughput engineering of the mouse genome coupled with high-resolution expression analysis. *Nat. Biotechnol.*, **21**, 652–659.
32. Song, H., Chung, S.-K. and Xu, Y. (2010) Modeling disease in human ESCs using an efficient BAC-based homologous recombination system. *Cell Stem Cell*, **6**, 80–89.
33. Frendewey, D., Chernomorsky, R., Esau, L., Om, J., Xue, Y., Murphy, A.J., Yancopoulos, G.D. and Valenzuela, D.M. (2010) The loss-of-allele assay for ES cell screening and mouse genotyping. *Methods Enzymol.*, **476**, 295–307.
34. Vajta, G., Zhang, Y. and Machaty, Z. (2007) Somatic cell nuclear transfer in pigs: recent achievements and future possibilities. *Reprod. Fertil. Dev.*, **19**, 403–423.
35. Spurney, C.F., Gordish-Dressman, H., Guerron, A.D., Sali, A., Pandey, G.S., Rawat, R., Van Der Meulen, J.H., Cha, H.J., Pistilli, E.E., Partridge, T.A. *et al.* (2009) Preclinical drug trials in the mdx mouse: assessment of reliable and sensitive outcome measures. *Muscle Nerve*, **39**, 591–602.
36. Yeung, E.W., Whitehead, N.P., Suchyna, T.M., Gottlieb, P.A., Sachs, F. and Allen, D.G. (2005) Effects of stretch-activated channel blockers on [Ca2+]i and muscle damage in the mdx mouse. *J. Physiol.*, **562**, 367–380.
37. Cooper, B.J. (2001) Animal models of human muscle disease. In Karpati, G., Hilton-Jones, D. and Griggs, R.C. (eds), *Disorders of Voluntary Muscle*. Cambridge University Press, Cambridge, pp. 187–216.
38. Tinsley, J.M., Potter, A.C., Phelps, S.R., Fisher, R., Trickett, J.I. and Davies, K.E. (1996) Amelioration of the dystrophic phenotype of mdx mice using a truncated utrophin transgene. *Nature*, **384**, 349–353.
39. Tinsley, J., Deconinck, N., Fisher, R., Kahn, D., Phelps, S., Gillis, J.M. and Davies, K. (1998) Expression of full-length utrophin prevents muscular dystrophy in mdx mice. *Nat. Med.*, **4**, 1441–1444.
40. Grady, R.M., Teng, H., Nichol, M.C., Cunningham, J.C., Wilkinson, R.S. and Sanes, J.R. (1997) Skeletal and cardiac myopathies in mice lacking utrophin and dystrophin: a model for Duchenne muscular dystrophy. *Cell*, **90**, 729–738.
41. Gramolini, A.O., Karpati, G. and Jasmin, B.J. (1999) Discordant expression of utrophin and its transcript in human and mouse skeletal muscles. *J. Neuropathol. Exp. Neurol.*, **58**, 235–244.
42. Sewry, C.A., Nowak, K.J., Ehmsen, J.T. and Davies, K.E. (2005) A and B utrophin in human muscle and sarcolemmal A-utrophin associated with tumours. *Neuromuscul. Disord.*, **15**, 779–785.
43. Lanfossi, M., Cozzi, F., Bugini, D., Colombo, S., Scarpa, P., Morandi, L., Galbiati, S., Cornelio, F., Pozza, O. and Mora, M. (1999) Development of muscle pathology in canine X-linked muscular dystrophy. I. Delayed postnatal maturation of affected and normal muscle as revealed by myosin isoform analysis and utrophin expression. *Acta Neuropathol.*, **97**, 127–138.
44. Nguyen, F., Cherel, Y., Guigand, L., Goubault-Leroux, I. and Wyers, M. (2002) Muscle lesions associated with dystrophin deficiency in neonatal golden retriever puppies. *J. Comp. Pathol.*, **126**, 100–108.
45. Lu, H., Huang, D., Ransohoff, R.M. and Zhou, L. (2011) Acute skeletal muscle injury: CCL2 expression by both monocytes and injured muscle is required for repair. *FASEB J.*, **25**, 3344–3355.
46. Litten-Brown, J.C., Corson, A.M. and Clarke, L. (2010) Porcine models for the metabolic syndrome, digestive and bone disorders: a general overview. *Animal*, **4**, 899–920.

47. Ashmore, C.R., Addis, P.B. and Doerr, L. (1973) Development of muscle fibers in the fetal pig. *J. Animal Sci.*, **36**, 1088–1093.
48. Karpati, G. and Carpenter, S. (1986) Small-caliber skeletal muscle fibers do not suffer deleterious consequences of dystrophic gene expression. *Am. J. Med. Genet.*, **25**, 653–658.
49. Grounds, M.D. and Shavlakadze, T. (2011) Growing muscle has different sarcolemmal properties from adult muscle: a proposal with scientific and clinical implications: reasons to reassess skeletal muscle molecular dynamics, cellular responses and suitability of experimental models of muscle disorders. *BioEssays*, **33**, 458–468.
50. Goemans, N.M., Tulinius, M., van den Akker, J.T., Burm, B.E., Ekhart, P.F., Heuvelmans, N., Holling, T., Janson, A.A., Platenburg, G.J., Sipkens, J.A. *et al.* (2011) Systemic administration of PRO051 in Duchenne's muscular dystrophy. *N. Engl. J. Med.*, **364**, 1513–1522.
51. Richter, A., Kurome, M., Kessler, B., Zakhartchenko, V., Klymiuk, N., Nagashima, H., Wolf, E. and Wuensch, A. (2012) Potential of primary kidney cells for somatic cell nuclear transfer mediated transgenesis in pig. *BMC Biotechnol.*, **12**, 84.
52. Kurome, M., Ueda, H., Tomii, R., Naruse, K. and Nagashima, H. (2006) Production of transgenic-clone pigs by the combination of ICSI-mediated gene transfer with somatic cell nuclear transfer. *Transgenic Res.*, **15**, 229–240.
53. Besenfelder, U., Modl, J., Muller, M. and Brem, G. (1997) Endoscopic embryo collection and embryo transfer into the oviduct and the uterus of pigs. *Theriogenology*, **47**, 1051–1060.
54. Trapnell, C., Pachter, L. and Salzberg, S.L. (2009) TopHat: discovering splice junctions with RNA-Seq. *Bioinformatics*, **25**, 1105–1111.
55. Trapnell, C., Williams, B.A., Pertea, G., Mortazavi, A., Kwan, G., van Baren, M.J., Salzberg, S.L., Wold, B.J. and Pachter, L. (2010) Transcript assembly and quantification by RNA-Seq reveals unannotated transcripts and isoform switching during cell differentiation. *Nat. Biotechnol.*, **28**, 511–515.
56. Cooper, S.T., Lo, H.P. and North, K.N. (2003) Single section Western blot: improving the molecular diagnosis of the muscular dystrophies. *Neurology*, **61**, 93–97.
57. Hermanns, W., Liebig, K. and Schulz, L.C. (1981) Postembedding immunohistochemical demonstration of antigen in experimental polyarthritis using plastic embedded whole joints. *Histochemistry*, **73**, 439–446.
58. Gundersen, H.J.G. (1977) Notes on the estimation of numerical density of arbitrary profiles: the edge effect. *J. Microsc. Oxford*, **111**, 219–223.
59. Briguet, A., Courdier-Fruh, I., Foster, M., Meier, T. and Magyar, J.P. (2004) Histological parameters for the quantitative assessment of muscular dystrophy in the mdx-mouse. *Neuromuscl. Disord.*, **14**, 675–682.
60. Weibel, E.R. (1979) *Stereological Methods I. Practical Methods for Biological Morphometry*. Academic Press, London.

平成24年度日本レーザー医学会総会賞受賞論文

AWARDED ARTICLE

生体二光子イメージングによる生活習慣病の分子機構と慢性炎症の寄与

西村　智[1,2]

[1]東京大学大学院医学系研究科 循環器内科
[2]東京大学 システム疾患生命科学による先端医療技術開発拠点

(平成25年5月10日受理，平成25年8月13日掲載決定)

In vivo Multi-Photon Molecular Imaging Visualizes Inflammatory and Immune Cell Cross-Talks in Adult Common Disease

Satoshi Nishimura[1,2]

[1]*Department of Cardiovascular Medicine, Graduate School of Medicine, The University of Tokyo, Japan*
[2]*Translational Systems Biology and Medicine Initiative, The University of Tokyo, Japan*

(Received May 10, 2013, Accepted August 13, 2013)

要　旨

最近の研究により各種生活習慣病の背景には，慢性炎症を基盤とした異常な細胞間作用が生体内で生じていることが明らかになっている．我々は，一光子・二光子レーザー顕微鏡を用いた「生体分子イメージング手法」を独自に開発し，生活習慣病にアプローチしてきた．著者らは，本手法を肥満脂肪組織に適応し，肥満脂肪組織で，脂肪細胞分化・血管新生が空間的に共存して生じ，また，脂肪組織微小循環では炎症性の細胞動態を生じている事を明らかにした．また，肥満脂肪組織にはCD8陽性T細胞が存在し肥満・糖尿病病態に寄与していた．さらに，本手法を用いて生体内の血栓形成過程の詳細も明らかになり，iPS由来の人工血小板の機能解析も可能となっている．

キーワード：生体イメージング，炎症，免疫細胞，二光子顕微鏡

Abstract

To elucidate the underlying mechanisms of adult common diseases based on chronic inflammation including metabolic and thrombotic disease, it is vital to examine the multi-cellular kinetics in living animals. Therefore, we developed in vivo imaging technique based on single- and multi-photon microscopy, and we assessed dynamic immune and inflammatory cellular interplay in diseased conditions. The power of our imaging technique to analyze complex cellular interplays in inflammatory diseases, especially parenchymal and stromal cell cross talks was eclucidated. It enabled us to evaluate new therapeutic interventions against adult common diseases.

Key words：*In vivo* imaging, inflammation, immune cells, two-photon microscopy

〒113－8655 東京都文京区本郷7－3－1　TEL / FAX 03－5800－5139
(7-3-1 Hongo, Bunkyo, Tokyo 113-8655, Japan)
Corresponding author: snishi-tky@umin.ac.jp（西村　智）

1. 緒言　なぜ生体イメージングなのか

心筋梗塞や脳卒中など動脈硬化性疾患の重大なリスク要因として，内蔵肥満とインスリン抵抗性を基礎とするメタボリックシンドロームが注目されている．肥満に伴い蓄積した内臓脂肪は多様なアディポサイトカインを分泌する等多彩な機能をもち，インスリン抵抗性や動脈硬化の発症に必須の役割を担っていると考えられる．しかし脂肪組織の肥満における役割は必ずしも明らかではなく，脂肪組織が臓器としてどのように機能異常を起こすのか，その分子機構はよく分かっていない．

最近の研究により，心筋梗塞や脳卒中などの原因となるメタボリックシンドロームと慢性炎症病態に密接な関連があることが示唆されている．メタボリックシンドロームでは，遺伝子素因と，内蔵肥満・加齢・喫煙などの外的誘因の両者が病態形成に関わっていることは，多くの臨床データから明らかである．しかし，慢性炎症そのものの動態が不明であることから，基礎病態に対する特効薬的な治療が存在せず，それに伴う生活習慣病病態については，多くの有疾患患者と高い死亡率を生んでいるのが現状である．そして，病態理解のためには，慢性炎症に伴う生体内での細胞動態の異常，特に免疫細胞の局所での生体内応答について，直接画像化して知見を得ることは必須であると言える．

2. 肥満と慢性炎症　生体分子イメージングでみる肥満脂肪組織

2.1 肥満脂肪組織における生体分子イメージングの意義

動脈硬化・心血管疾患の原因として，末梢組織（骨格筋・脂肪組織）の機能異常が重要であると考えられるようになった．特に，脂肪組織は，長年，脂肪を蓄積するのみの「何もしない臓器」と考えられてきた．近年のライフスタイルの変化（食生活の欧米化）に伴う肥満・メタボリックシンドロームの蔓延により，脂肪組織は，様々な病気を引き起こす「活発な代謝臓器」として一躍，注目を浴びるようになったしかし，脂肪組織の肥満における役割は必ずしも明らかではなく，脂肪組織が臓器としてどのように機能異常を起こすのか，その分子機構は十分解明されているとは言えない．近年の Weisberg らによる肥満脂肪組織に炎症性マクロファージが浸潤の報告[1]を初めとして，肥満脂肪組織における慢性炎症の関わりについては複数のグループが報告しており，現在では肥満脂肪組織のリモデリングの背景に慢性炎症が存在することは明らかと考えられている[2]．しかし，従来の切片標本を用いた組織観察では，脂肪組織における血管や組織間質に存在する細胞群の三次元的構造の詳細は観察不能であり，炎症が引き起こす生体内の細胞動態も不明であった．我々はメタボリックシンドロームの病態解明を目指し，新たに開発したイメージング手法を用いて，肥満に伴う脂肪組織の再構築（リモデリング）と機能異常を検討した．

2.2「生組織イメージング」でみる肥満脂肪組織リモデリング

我々はまず，「脂肪組織をよりよくみるために」，レーザー共焦点顕微鏡を用いて，生きたままの組織をそのまま染色する，「生組織イメージング手法」を開発した．

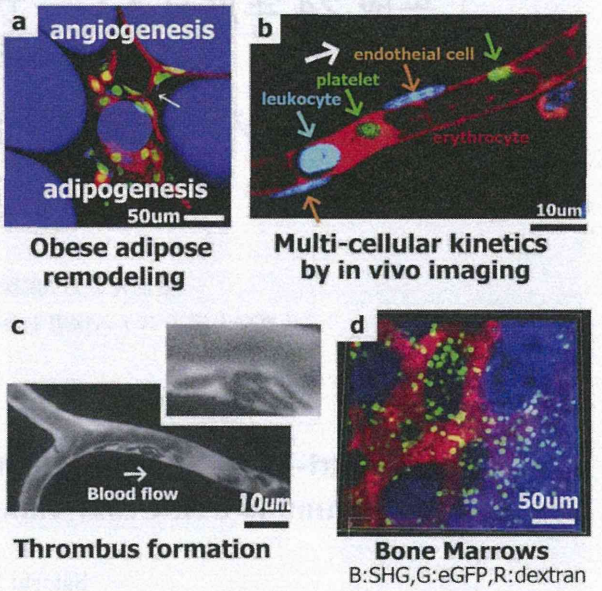

Fig.1 (a) Adipose tissue remodeling in obesity including adipogenesis and angiogenesis (b) Multi-cellular kinetics visualized by novel *in vivo* imaging technique (c) Thrombus formation and single platelet kinetics revealed by *in vivo* imaging (d) T cell proliferations in bone marrows after transplantation.

通常の固定した組織切片標本では，脂肪組織は白く抜けた脂質と，細胞質・核の集合体として漠然としか組織構築が捉えられなかったが，我々の手法では組織構築の詳細が可視化された[3]．

肥満動物モデルの脂肪組織では，多くの脂肪細胞は肥大していたが，加えて分化・増殖した小型脂肪細胞が新たに出現していた（Fig.1a）[3]．さらに，小型脂肪細胞分化と共存して血管新生像（血管網より枝分かれした新生血管の断端）が観察され，その周囲には活性化マクロファージ浸潤が認められた．我々は，この細胞集団を「adipo/angiogenic cell clusters」と名付けた．肥満に伴い脂肪組織の中では血管新生と脂肪細胞が空間的に共存し，脂肪組織のリモデリングを来していることが明らかになった．そしてこれらに対する介入実験として，血管新生の阻害を肥満動物に対して行ったところ，脂肪組織のなかの血管新生部位のみならず，脂肪細胞分化そのものも抑制された．阻害に伴い，全身の内臓肥満やインスリン抵抗性が改善し，肥満脂肪組織の病態形成に血管新生が必須であることが示唆された．

2.3 生体内の脂肪組織の可視化 生体分子イメージングの開発

従来，肥満に伴って脂肪組織内で慢性炎症が起きていることが示唆されていたが，その詳細な機序は不明であった．そこで，我々は本イメージング手法を生体に応用し「生きた動物の体内を手に取るように可視化すること」に成功し，肥満組織において炎症性の細胞動態が生じていることを可視化手法により明確に示している[4]．動脈硬化のように血管が主な傷害の場になる病態だけでなく，

腫瘍やメタボリックシンドロームにおいても，血流や血管機能といった生体内のダイナミックな変化，組織学的変化に先行する初期の炎症性変化を捉えることが可能な生体内分子イメージング技術は非常に有用である．従来の生体内観察では，透過光による観察が容易な腸間膜の微小循環を用いた研究が主に行われてきたが，近年の光学観察系・蛍光プローブの開発により，蛍光物質をトレーサーとして，透過光観察が不可能な厚みを有する脂肪組織をはじめとする実質臓器の血流観察も可能になった．時間・空間解像度も飛躍的に改善し，細胞内小器官レベルでの解析が可能となっている．

2.4 肥満脂肪組織と慢性炎症

我々は生体内分子イメージング手法を肥満内臓脂肪組織に応用することにより，脂肪組織内の微小血管で炎症性変化が起きていることを明らかにした．すなわち，肥満動物の白色脂肪組織内微小循環の観察で，細静脈レベルにおいて血管壁への白血球の接着・回転・血管外漏出運動が有意に増加していることをイメージングにより示した[4]．肥満脂肪組織中では血流が間歇的に低下し，低酸素状態である事も確認された．また，白血球の血管壁への付着には接着分子の発現増加と，活性化血小板の付着が伴っていた．すなわち，動脈硬化病変で知られているような炎症性の細胞動態が，肥満した脂肪組織の微小循環でも認められており，「肥満脂肪組織そのものが炎症の場である」ことが可視化手法により明確に示された．本イメージングでは単一血小板も生体内で捉えられており，血栓形成の詳細を可視化することも可能でになっている（後述）．

2.5 CD8陽性T細胞の重要性 肥満病態の最も初期のトリガーは何か？

我々は，分子イメージング及びFACS (fluorescence activated cell sorting, フローサイトメーター) を用いたハイスループットの解析から，脂肪組織の間質に多くのリンパ球が存在することも明らかにした．痩せ形マウスでも間質細胞の約10%はT細胞であり，肥満に伴ってその数は増加する．T細胞は表面マーカーの発現，機能（サイトカイン産生能など）により，主に，CD8，CD4陽性T細胞にわけられる．T細胞サブセットの解析では，肥満に伴い，CD8陽性T細胞の増加，CD4陽性T細胞・制御性T細胞の減少が認められた[5]．我々以外のグループでは，Winerらは T細胞を標的とした免疫療法によりマウスの肥満が改善することを示している[6]．また，脂肪組織にはマスト細胞・制御性T細胞といった特有のT細胞が存在し，局所免疫や脂肪組織炎症をコントロールし，肥満に伴うインスリン抵抗性に寄与している事も明らかになった[7,8]．このように脂肪組織局所においてはマクロファージやT細胞をはじめとする多様な細胞が相互作用し，メタボリックシンドロームの病態を形成していると考えられる．我々はCD8陽性T細胞の役割を明らかにするため，CD8ノックアウトマウスおよび中和抗体を用いた検討，及び，複数の細胞種を用いた *in vitro* での共培養の実験を行った．すなわち，肥満脂肪組織ではCD8陽性T細胞がポリクローナルに活性化・増殖しており，このCD8陽性T細胞は骨髄由来の単球からマクロファージへの分化，および，マクロファージの肥満脂肪組織への遊走・活性化を促進していた．このCD8陽性T細胞は一部は骨髄由来であることが移植実験により確かめられている．つまり，肥満脂肪組織における炎症性マクロファージ浸潤の初期のトリガーがCD8陽性T細胞の浸潤であることが示唆された．異常な肥満脂肪組織における局所免疫が，全身及び肥満脂肪組織の炎症，さらに糖尿病病態を引き起こしていることが示された．また，ヒトサンプルにおいても，肥満者の脂肪組織においてCD8遺伝子が高発現となることから，CD8陽性T細胞はマウスのみならず，ヒトにおいても重要な役割を持つことが示唆されている．

3. 血小板機能の生体イメージングを用いた可視化

本邦の死因の上位を占める脳・心血管イベントの多くは血管の動脈硬化性変化を基盤としている．例えば，血栓性疾患（アテローム血栓症）では慢性炎症病態を基盤とした動脈硬化巣の形成と，それに引き続いて起こる，粥腫（アテローム）の破綻が病態形成に重要である．破綻部位においては，血小板は活性化され，血小板血栓が形成される他，凝固系も病態に関与する．しかし，動脈硬化巣の破綻は偶発的かつ高速に進行する病態であり，実験的にこれらを *ex vivo*, *in vitro* で再現することは不可能であった．実際に，これらの一連の過程には血小板のみならず，各種炎症性細胞，血管内皮細胞とその障害，局所の血流動態（血流とずり応力）が関わっている．このような多細胞からなる複雑病変とそのダイナミクスが病態の本質であり，これらを生体内で検討する手法が，病態理解の上で求められており，その検討を可能にしたのが我々の開発した「生体分子イメージング手法」である．

血小板をFITC-Dextran及びanti-CD41，anti-GPIb抗体により可視化したところ，定常状態においては，細動脈・静脈では血管壁近傍にそって血小板は運動していた．一方，流速の遅い毛細血管のレベルでは，血小板は血管内皮と相互作用して「stop and go」を繰り返しており，血流にのって回転運動しながら流れているさまが可視化された．さらに，レーザー照射・傷害と組み合わせる事で血栓形成を誘発し，生体内での単一血小板を捉えながら，血栓形成のメカニズムの詳細が可視化された (Fig.1c)．

我々の血栓形成モデルでは，まずレーザー照射により活性酸素の産生が誘発されて血管内皮に血小板が付着する．その後，血小板はその数を増やし積み上がり，血管内腔を狭小化し，血液の流速は遅くなる．その後，赤血球，もしくは，白血球により血管は閉塞する．本モデルが特徴的なのは，血栓形成の全過程が数十秒で終わり，時間的に経過がきわめて早い事である．本モデルではレーザー照射後に血栓形成に寄与した血小板数を数えることにより血栓形成能が定量可能であり，従来の頸動脈に対する塩化鉄傷害モデルにおける血栓による閉塞時間とも強い相関を示しており，生体内の血小板機能をきわめて鋭敏に示していると考えられる．それだけでなく，従来の止血時間の計測では分からなかった，血栓形成の素過程が可視化されており，遺伝子改変の効果がどの過程に影

響を及ぼしているかを明らかにすることが出来る.

我々は本手法を用いて,Lnkというアダプター蛋白に注目して実験を進めた.Lnkは血球系幹細胞の維持に重要な蛋白であるが,巨核球・血小板にも発現している.興味深い事に,Lnkの欠損した遺伝子改変動物では,流血中の末梢血小板数が野生型の5倍になるにもかかわらず血栓性を示さず,むしろ止血時間が延長しており,Lnkの欠損が血小板機能に影響をもたらしていると考えた.骨髄移植を行い作成したLnkキメラマウスを用い,生体イメージングにより血栓形成過程を観察したところ,血球系でのみLnkが欠損したLnkキメラマウスではレーザー傷害により血小板は血管内皮に付着するものの,血栓は安定化・piling upせず血流に押し流され,血小板血栓の発達が阻害されていた.すなわち,Lnkが血小板血栓の安定化に寄与している事が示された.分子生物学的機序としてはインテグリンのシグナリングにリン酸化したLnkがC-Src,Fynなどと協同して関与していた[9].以上よりLnkが生体内血栓の形成・安定化に寄与していることが明確に示された.

近年,Lnkの遺伝子変異がヒトにおいて多血症・血小板無力症や骨髄増殖性疾患を引き起こすことも報告されている[10,11].多血症では血小板数は増加するものの,血小板機能は低下していることが多く,今回,Lnkノックアウトマウスでみられた表現型にきわめて近いと言え,Lnkの血小板機能における重要性がマウスだけでなく,ヒトにおいても示されている.

さらに,炎症性サイトカインのノックアウトマウス,キメラマウスの解析の結果,TNF-αをはじめとする炎症性サイトカインが,ROS(Reactive Oxygen Species,活性酸素)刺激下でのvWF因子(von willebrand factor,フォンヴィルブランド因子)の血管内皮表面への表出に関わっていることが明らかになった.ROSは血管内皮を障害し軽度の炎症状態を誘導する.その結果,血小板と血管内皮の相互作用に重要な蛋白であるvWF因子を血管内皮表面に誘導する.さらに,IL-1,IL-6等の因子も血栓性を促進しており,これらの炎症性サイトカインは血管内皮に作用し,インテグリンシグナルと協同して,血栓の安定化に寄与していた.従来,炎症と血栓については多様な報告によりその関連が示唆されていたが,本解析により血栓形成過程のうち,血管内皮における炎症性サイトカインのシグナリングが血栓形成に関わっていることが示された[12].

今後は,さらに様々な血小板機能に異常を来す遺伝子改変動物における血栓形成過程・血小板動態を観察することにより,「生体内の血栓形成の各過程における遺伝子・物質の関与」を検討していきたい.

4. iPS由来人工血小板の体内イメージング

近年の,多能性幹細胞(ES,iPS)の研究の進歩により,細胞療法を含む再生医学での広い範囲での臨床応用が期待されている.しかし,これらの基礎研究を臨床に繋げるためには,ヒトを対象とした研究に移行する前に,実際に試験管内で作成した細胞が,実際の個体(マウス及び大動物)の中でどのように機能しているか,どのように病変に働くかを明らかにすることは必須である.しかし,今までこれらiPS由来の分化誘導細胞の体内での細胞動態を検討する手法は存在しなかった.共同研究者の東京大学医科学研究所幹細胞治療分野江藤准教授チームはC-Mycの発現をコントロールすることにより,飛躍的に効率的に,ヒトiPS由来の人工血小板を作成する手法を確立した.我々は生体イメージングを用いて,こうして得られたヒトiPS由来血小板の体内動態の可視化を行った.観察に用いて免疫不全マウス(NOGマウス)の体内で,iPS由来血小板の細胞動態が捉えられ,iPS由来血小板がマウス体内を循環しているだけでなく,レーザー傷害により誘発された血栓形成部位においてはホスト血小板とiPS由来血小板が相互作用しながら血栓を形成するさまが観察された.つまり「人工血小板は体内を循環し,血栓も作る」事が証明されたわけである.本イメージング手法はiPS分化誘導細胞を用いた細胞療法の臨床応用にむけて,安全性・有用性を評価する上できわめて有用性が高い手法と言える[13].

5. 次世代のイメージング 深部を照らす機能イメージング

我々は主にニポウ式レーザー共焦点,一光子励起の組み合わせで画像取得を行ってきた.しかし,深部臓器・臓器内部の構造に関しては可視化できず,遺伝子機能も不明であった.生体の各種病態下での細胞連関・情報伝達異常をより明らかにするためには,形態と機能と組み合わせた深部の光イメージングが今後必要になると考えられる.例えば,遺伝子改変動物を用いた遺伝子機能の光による解析を,二光子フェムト秒レーザーと高速スキャニング共焦点システムで行うというものであり,今後の光学機器の開発・改良が望まれる.

利益相反の開示

利益相反なし.

参考文献

1) S.P. Weisberg, D. McCann, M. Desai, M. Rosenbaum, R.L. Leibel, A.W. Ferrante: Obesity is associated with macrophage accumulation in adipose tissue, J. Clin. Invest., 112(12): 1796-1808, 2003.
2) G.S. Hotamisligil: Inflammation and metabolic disorders Nature, 444 (7121): 860-867, 2006.
3) S. Nishimura, I. Manabe, M. Nagasaki, Y. Hosoya, H. Yamashita, H. Fujita, M. Ohsugi, K. Tobe, T. Kadowaki, R. Nagai, S. Sugiura: Adipogenesis in obesity requires close interplay between differentiating adipocytes, stromal cells, and blood vessels, Diabetes, 56: 1517-1526, 2007.
4) S. Nishimura, I. Manabe, M. Nagasaki, K. Seo, H. Yamashita, Y. Hosoya, M. Ohsugi, K. Tobe, T. Kadowaki, R. Nagai, S. Sugiura: *In vivo* imaging in mice reveals local cell dynamics and inflammation in obese adipose tissue, J. Clin. Invest., 118(2): 710-721, 2008.
5) S. Nishimura, I. Manabe, M. Nagasaki, K. Eto, H. Yamashita, M. Ohsugi, M. Otsu, K. Hara, K. Ueki, S. Sugiura, K. Yoshimura, T. Kadowaki, R. Naga: CD8+ effector T cells contribute to macrophage recruitment and adipose tissue inflammation in obesity, Nature Medicine, 15(8): 914-920, 2009.

6) S. Winer, Y. Chan, G. Paltser, D. Truong, H. Tsui, J. Bahrami, R. Dorfman, Y. Wang, J. Zielenski, F. Mastronardi, Y. Maezawa, D.J. Drucker, E. Engleman, D. Winer, H.M. Dosch: Normalization of obesity-associated insulin resistance through immunotherapy, Nature Medicine, 15(8): 921-929, 2009.
7) J. Liu, A. Divoux, J. Sun, J. Zhang, K. Clement, J.N. Glickman, G.K. Sukhova, P.J. Wolters, J. Du, C.Z. Gorgun, A. Doria, P. Libby, R.S. Blumberg, B.B. Kahn, G.S. Hotamisligil, G.P. Shi: Genetic deficiency and pharmacological stabilization of mast cells reduce diet-induced obesity and diabetes in mice., Nature Medicine, 15(8): 940-945, 2009.
8) M. Feuerer, L. Herrero, D. Cipolletta, A. Naaz, J. Wong, A. Nayer, J. Lee, A.B. Goldfine, C. Benoist, S. Shoelson, D. Mathis: Lean, but not obese, fat is enriched for a unique population of regulatory T cells that affect metabolic parameters. Nature Medicine, 15(8): 930-939, 2009.
9) S. Nishimura, H. Takizawa, N. Takayama, A. Oda, H. Nishikii, Y. Morita, S. Kakinuma, S. Yamazaki, S. Okamura, N. Tamura, S. Goto, A. Sawaguchi, I. Manabe, K. Takatsu, H. Nakauchi, S. Takaki, K. Eto: Lnk/Sh2b3 regulates integrin alpha-IIb-beta3 outside-in signaling in platelets leading to stabilization of developing thrombus *in vivo*. J. Clin. Invest., 120(1): 179-190, 2010.
10) S.T. Oh, E.F. Simonds, C. Jones, M.B. Hale, Y. Goltsev, K.D. Gibbs Jr, J.D. Merker, J.L. Zehnder, G.P. Nolan, J. Gotlib: Novel mutations in the inhibitory adaptor protein LNK drive JAK-STAT signaling in patients with myeloproliferative neoplasms.Blood 116(6): 988-992, 2010.
11) T.L. Lasho, A. Pardanani, A. Tefferi: LNK mutations in JAK2 mutation-negative erythrocytosis. N. Engl. J. Med., 363(12): 1189-1190, 2010.
12) S. Nishimura, I. Manabe, M. Nagasaki, S. Kakuta, Y. Iwakura, N. Takayama, J. Ooehara, M. Otsu, A. Kamiya, B. Petrich, T. Urano, T. Kadono, S. Sato, A. Aiba, H. Yamashita, S. Sugiura, T. Kadowaki, H. Nakauchi, K. Eto, R. Nagai: *In vivo* imaging visualizes discoid platelet aggregations without endothelium disruption and implicates contribution of inflammatory cytokine and integrin signaling. Blood., 119(8): e45-56, 2012.
13) N. Takayama, S. Nishimura, S. Nakamura, T. Shimizu, R. Ohnishi, H. Endo, T. Yamaguchi, M. Otsu, K. Nishimura, M. Nakanishi, A. Sawaguchi, R. Nagai, K. Takahashi, S. Yamanaka, H. Nakauchi, K. Eto: Transient activation of c-MYC expression is critifal for efficient platelet generation from human induced pluripotent stem cells. J. Exp. Med., 207(13): 2817-2830, 2010.

著者紹介

西村　智（Satoshi Nishimura）
1999年3月，東京大学医学部医学科 卒業．2006年4月，日本学術振興会 特別研究員（DC2）．2007年4月，東京大学大学院医学系研究科博士課程 修了(医学博士，内科学専攻)．同年4月，日本学術振興会 特別研究員（PD）．2008年10月，東京大学大学院医学系研究科循環器内科 特任助教，科学技術振興機構さきがけ「光の利用と物質材料・生命機能」研究員（兼任）．同年11月，東京大学医療ナノテク人材育成ユニット 特任助教．2009年4月，東京大学システム疾患生命科学による先端医療技術開発拠点（TSBMI）特任助教．2011年10月，同 特任准教授，現在に至る．

日本内科学会，日本循環器学会，日本心臓病学会 糖尿病学会，日本バイオイメージング学会（評議員），日本肥満学会，日本医用画像工学会，日本血管生物医学会，日本分子イメージング学会，日本内分泌学会，日本心血管内分泌代謝学会，日本分子生物学会，日本顕微鏡学会，日本糖尿病動物研究会，バイオインダストリー協会，日本微小循環学会，日本炎症・再生医学会，他多数．

Generating Porcine Chimeras Using Inner Cell Mass Cells and Parthenogenetic Preimplantation Embryos

Kazuaki Nakano[1], Masahito Watanabe[2], Hitomi Matsunari[2], Taisuke Matsuda[1], Kasumi Honda[1], Miki Maehara[1], Takahiro Kanai[1], Gota Hayashida[1], Mirina Kobayashi[1], Momoko Kuramoto[1], Yoshikazu Arai[1], Kazuhiro Umeyama[2], Shuh-hei Fujishiro[3], Yoshihisa Mizukami[3], Masaki Nagaya[2], Yutaka Hanazono[3,4], Hiroshi Nagashima[1,2]*

1 Laboratory of Developmental Engineering, Department of Life Sciences, School of Agriculture, Meiji University, Kawasaki, Japan, **2** Meiji University International Institute for Bio-Resource Research (MUIIBR), Kawasaki, Japan, **3** Division of Regenerative Medicine, Center for Molecular Medicine, Jichi Medical University, Tochigi, Japan, **4** CREST, Japan Science and Technology Agency, Tokyo, Japan

Abstract

Background: The development and validation of stem cell therapies using induced pluripotent stem (iPS) cells can be optimized through translational research using pigs as large animal models, because pigs have the closest characteristics to humans among non-primate animals. As the recent investigations have been heading for establishment of the human iPS cells with naïve type characteristics, it is an indispensable challenge to develop naïve type porcine iPS cells. The pluripotency of the porcine iPS cells can be evaluated using their abilities to form chimeras. Here, we describe a simple aggregation method using parthenogenetic host embryos that offers a reliable and effective means of determining the chimera formation ability of pluripotent porcine cells.

Methodology/Significant Principal Findings: In this study, we show that a high yield of chimeric blastocysts can be achieved by aggregating the inner cell mass (ICM) from porcine blastocysts with parthenogenetic porcine embryos. ICMs cultured with morulae or 4–8 cell-stage parthenogenetic embryos derived from *in vitro*-matured (IVM) oocytes can aggregate to form chimeric blastocysts that can develop into chimeric fetuses after transfer. The rate of production of chimeric blastocysts after aggregation with host morulae (20/24, 83.3%) was similar to that after the injection of ICMs into morulae (24/29, 82.8%). We also found that 4–8 cell-stage embryos could be used; chimeric blastocysts were produced with a similar efficiency (17/26, 65.4%). After transfer into recipients, these blastocysts yielded chimeric fetuses at frequencies of 36.0% and 13.6%, respectively.

Conclusion/Significance: Our findings indicate that the aggregation method using parthenogenetic morulae or 4–8 cell-stage embryos offers a highly reproducible approach for producing chimeric fetuses from porcine pluripotent cells. This method provides a practical and highly accurate system for evaluating pluripotency of undifferentiated cells, such as iPS cells, based on their ability to form chimeras.

Citation: Nakano K, Watanabe M, Matsunari H, Matsuda T, Honda K, et al. (2013) Generating Porcine Chimeras Using Inner Cell Mass Cells and Parthenogenetic Preimplantation Embryos. PLoS ONE 8(4): e61900. doi:10.1371/journal.pone.0061900

Editor: Qiang Wu, National University of Singapore, Singapore

Received November 24, 2012; **Accepted** March 15, 2013; **Published** April 23, 2013

Funding: This work was supported by the Core Research for Evolutional Science and Technology (CREST) of the Japan Science and Technology Agency and by the Meiji University International Institute for Bio-Resource Research (MUIIBR). The funders had no role in study design, data collection and analysis, decision to publish, or preparation of the manuscript.

Competing Interests: The authors have declared that no competing interests exist.

* E-mail: hnagas@isc.meiji.ac.jp

Introduction

In recent years, dramatic progress has been made in research into the application of induced pluripotent stem (iPS) cells for the treatment of both intractable genetic diseases and acquired disorders such as myocardial infarction [1], macular degeneration [2,3] and spinal injury [4]. However, before iPS cells can be used for clinical therapies, extensive animal experiments are necessary to elucidate therapeutic mechanisms and to evaluate the efficacy and safety of potential treatments. Although a range of experimental animal models is available, it is preferable that such investigations are conducted on those with anatomical and physiological similarities to humans. For this reason, pigs are often chosen for use in translational research because they possess the closest similarity to humans among non-primate animal models [5,6], and consequently, the results of research on porcine iPS cell therapy [7,8] can be more easily extrapolated to humans.

Recent investigations have been heading for establishment of human iPS cell with naïve state characteristics [9–11]. Similarly, development of the naïve type porcine iPS cells [12] has become an important challenge in translational research using pigs, since the pioneering works on porcine iPS cells [7,12–16]. Thus, the pluripotency of porcine iPS cells need to be evaluated by a reliable means. Authentic pluripotency of the iPS cells can be proven by their competence to contribute to chimera formation. To date,

however, the ability of porcine iPS cells to form chimeras is still very limited. In general, the methods used to judge whether established pluripotent cells possess the ability to form chimeras evaluate the success of incorporation of sample cells (donor cells) into developing host embryos and their contribution to the fetus or offspring. This is a lengthy and involved test procedure and has stimulated a search for more simple and efficient methods for proving pluripotency.

The incorporation of donor cells into a host embryo can be achieved either by injecting donor cells directly into the blastocoele of a host blastocyst [17] or by an aggregation method in which donor cells are co-cultured with the host embryo [18,19]. Although the former method has been used successfully to show the ability of donor cells to form chimeras [12,15,20–26], the method requires a high skill level and expensive equipments. In contrast, the aggregation method offers a simple approach to generating chimeric embryos [27].

There have been a number of advances in pig reproductive technologies in recent years, including *in vitro* oocyte maturation, parthenogenetic oocyte activation, and *in vitro* embryo culture [28–30]. These developments have made it possible to culture parthenogenetic embryos to the somite stage [31–33]. Consequently, it is now feasible to use a parthenogenetic embryo as the host for the evaluation of the ability of pluripotent cells to form chimeric fetuses. The use of parthenogenetic embryos derived from *in vitro*-matured (IVM) oocytes offers the additional advantage of saving labor and costs compared to the use of *in vivo*-derived embryos.

In the present study, we demonstrate that the aggregation method can be used with parthenogenetic porcine embryos derived from IVM oocytes to efficiently generate chimeric embryos and fetuses with pluripotent cells. This system provides a simple and reliable means for evaluating the pluripotency of established iPS cell lines through comparison of their abilities to form chimeric embryos.

Methods

Animal Care

The pigs used in the present study were maintained in a semiwindowless facility with a controlled temperature (15–30°C) and received a standard pig diet twice a day and water *ad libitum*. All of the animal experiments in the present study were approved by the Institutional Animal Care and Use Committee of Meiji University (IACUC-11-1).

Chemicals

Chemicals were purchased from the Sigma Chemical Co. (St. Louis, MO, USA), unless otherwise indicated.

In vitro Oocyte Maturation

IVM oocytes were prepared as described elsewhere [34]. Pig ovaries were collected at a local abattoir and transported to the laboratory in Dulbecco's phosphate-buffered saline (DPBS; Nissui Pharmaceutical Co., Ltd., Tokyo, Japan) containing 75 μg/ml potassium penicillin G, 50 μg/ml streptomycin sulfate, 2.5 μg/ml amphotericin B and 0.1% (w/v) polyvinyl alcohol (PVA). Cumulus-oocyte complexes (COCs) were collected by aspiration from ovarian antral follicles that had a diameter of 3.0–6.0 mm. COCs with at least three layers of compacted cumulus cells were selected and culture in NCSU23 medium [35] supplemented with 0.6 mM cysteine, 10 ng/ml epidermal growth factor, 10% (v/v) porcine follicular fluid, 75 μg/ml potassium penicillin G, 50 μg/ml streptomycin sulfate, 10 IU/ml eCG (ASKA Pharmaceutical Co., Ltd., Tokyo, Japan) and 10 IU/ml hCG (ASKA Pharmaceutical). The COCs were cultured for 22 hr with eCG and hCG in a humidified atmosphere of 5% CO_2 and 95% air at 38.5°C. The COCs were then cultured for 22 hr without eCG and hCG in an atmosphere of 5% CO_2, 5% O_2 and 90% N_2 [36]. IVM oocytes with expanded cummulus cells were treated with 1 mg/ml hyaluronidase dissolved in Tyrode's lactose medium containing 10 mM Hepes and 0.3% (w/v) polyvinylpyrrolidone (Hepes-TL-PVP) and were separated from the cumulus cells by gentle pipetting. Oocytes with an evenly granulated ooplasm and an extruded first polar body were selected for subsequent experiments.

Parthenogenetic Activation of Oocytes

Parthenogenetic embryos developed from IVM oocytes were used as host embryos in all the experiments. Parthenogenesis of oocytes was induced by electric activation as reported previously [34]. The oocytes were washed twice in an activation solution composed of 280 mM mannitol (Nacalai Tesque, Inc., Kyoto, Japan), 0.05 mM $CaCl_2$, 0.1 mM $MgSO_4$ and 0.01% (w/v) PVA. They were then aligned between two wire electrodes (1.0 mm apart) in a drop of the activation solution on a fusion chamber slide (CUY500G1, Nepa Gene, Chiba, Japan). A single direct current pulse of 150 V/mm was applied for 100 μsec using an electrical pulsing machine (LF201; Nepa Gene). Activated oocytes were treated with 5 μg/ml cytochalasin B for 3 hr to suppress extrusion of the second polar body.

In vitro Fertilization of Oocytes

Donor embryos for producing chimeric fetuses were prepared by *in vitro* fertilization of oocytes using frozen sperm of a transgenic boar carrying humanized Kusabira-Orange (huKO) gene. *In vitro* fertilization was carried out as described elsewhere [37]. Briefly, frozen epididymal sperm [38] recovered from a straw were suspended in 5 ml DPBS supplemented with 0.1% BSA (306–1138, Wako Pure Chemical industries, Ltd., Osaka, Japan) and washed three times by centrifugation at 1,000×g for 4 min. After washing, the sperm pellets were resuspended in porcine fertilization medium (PFM) [39] (Research Institute for the Functional Peptides, Yamagata, Japan) at a concentration of 1×10^7 cells/ml. For insemination, 20 COCs that had been matured *in vitro* were placed in a 100-μl drop of PFM containing spermatozoa (1.75×10^6 cells/ml); the oocytes and sperm were incubated for 8 hr at 38.5°C in a humidified atmosphere containing 5% CO_2, 5% O_2, and 90% N_2. After insemination, the eggs were transferred to Hepes-TL-PVP; cumulus cells and excess sperm were removed by gentle pipetting. Eggs that showed release of polar bodies with normal cytoplasmic morphology were selected for use in later experiments.

In vitro Culture of Embryos

In vitro culture of the parthenogenetic and *in vitro*-fertilized (IVF) embryos was performed in droplets of porcine zygote mediume-5 (PZM-5) (Research Institute for Functional Peptides) under paraffin oil (32033-00, Kanto Chemical Co., Inc., Tokyo, Japan) in plastic 35-mm dish maintained in a humidified atmosphere of 5% O_2 and 90% N_2 at 38.5°C. The culture media were supplemented with 10% (v/v) fetal calf serum for culturing embryos at the morula stage or later.

Isolation of Donor ICMs from Blastocysts

Donor ICMs were isolated from the parthenogenetic and IVF blastocysts by immunosurgery as described previously [22].

Briefly, day-6 blastocysts were incubated at 38.5°C for 15 min with heat-inactivated rabbit anti-pig spleen cell serum (BioTools Inc., Gunma, Japan) diluted 1:8 with 21 mM Hepes-buffered Minimal Essential Medium with Earle salts, L-glutamine and nonessential amino acids (Gibco-Invitrogen, Carlsbad, CA, USA) supplemented with 5 mg/ml BSA (MEM-Hepes). Embryos were then incubated with guinea pig complement serum, diluted 1:8 with MEM-Hepes at 38.5°C for 10–15 min. Swollen trophectodermal cells were dissociated by vigorous pipetting (inner diameter, 100 μm). The ICM was washed thoroughly with MEM-Hepes.

Isolation of Donor Blastomeres from Parthenogenetic Embryos

Blastomeres isolated from parthenogentic embryos were also used as donor cells to produce chimeric blastocysts. The parthenogenetic embryos at the 4–8 cell (day 3) or morula (day 4) stage were decompacted by incubation in Ca^{2+}/Mg^{2+}-free DPBS containing 0.1 mM EDTA-2Na and 0.01% (w/v) PVA for 15–20 min, followed by removal of the zona pellucidae by digesting with 0.25% (w/v) pronase (in DPBS). Blastomeres were isolated from the zona removed embryos by gentle pipetting with a finely drawn glass capillary.

Staining of Donor Cells for in vitro Tracing

Donor-ICMs and donor-blastomeres isolated from parthenogenetic embryos were labeled with fluorescent carbocyanine dye (DiI) (Takara Bio, Inc., Shiga, Japan) for tracing during the formation of chimeric blastocysts *in vitro*. Staining of the cells was performed according to the manufacturer's protocol. ICMs and blastomeres were placed in MEM-Hepes containing 1% (v/v) DiI for 30 min, after which excess DiI was washed out by immersing the cells twice in MEM-Hepes for 10 min each time.

Preparation of Chimeric Embryos

Aggregation of donor cells and host embryos was carried out using the micro-well method [40]. A cluster of 9 to 12 depressions (400 μm in diameter, 300 μm in depth) was made on the bottom of a culture dish (Iwaki 1000-35, Asahi Techno Glass, Tokyo, Japan) using an aggregation needle (BLS, Ltd., Budapest, Hungary) (Figure 1). The cluster of micro-wells was overlaid with a microdrop (30 μl) of PZM-5 and covered with paraffin oil.

Blastomeres of the host embryos were isolated from parthenogenetic morulae (day 4) and 4–8 cell stage embryos (day 3) by the same way for the donor cells as described above.

We first examined the *in vitro* development of chimeric embryos composed of the donor ICM and host blastomeres (Figure 1). A donor ICM of parthenogenetic blastocysts was placed in each micro-well with blastomeres isolated from two host embryos (Figure 2A, D).

As a control experiment, some of the ICMs were injected into host morulae. Isolated ICMs were inserted into the center portion of the host morulae (Figure 2G) using a beveled injection pipette by micromanipulation with a micromanipulator (MO-102, Narishige, Tokyo, Japan) and injectors (IM-6, Narishige).

In vitro development of chimeric embryos was also analyzed using donor blastomeres instead of donor ICMs (Figure 3). Blastomeres isolated from a parthenogenetic donor embryo at the morula or 4–8 cell stage were aggregated with the host blastomeres of an embryo at the synchronous or asynchronous stage.

Evaluation of Chimeric Blastocysts by Confocal Fluorescence Microscopy

Embryos produced by the aggregation method and those produced by ICM-injection were cultured for 48 to 72 hr to examine their ability to form chimeric blastocysts. Day-6 blastocysts were observed by confocal microscopy to determine contribution of the donor cells into the ICM. Blastocysts showing fluorescent signals in the ICM were judged to be chimeric. Images of blastocysts placed in a drop of DPBS containing 5 μg/ml Hoechst 33342 in the 35-mm glass-bottom dish (Iwaki 3910-035, Asahi Techno Glass) were taken by a confocal fluorescence microscope (FV-1000, Olympus, Tokyo, Japan) with 10-μm optical sections.

Generation of Chimeric Fetuses

To test whether the blastocysts generated by the aggregation method can give rise to chimeric fetuses, embryo transfer experiments were conducted (Figure 1). Donor ICMs derived from IVF blastocysts were aggregated with host blastomeres isolated from two parthenogenetic embryos at the morula or 4–8 cell stage. Aggregated embryos were cultured for 1 to 2 days, and blastocysts obtained were transferred to recipient gilts. Pregnant recipients were laparotomized to recover somite stage fetuses at day 18 of gestation.

Blastocysts (day 5 and 6) obtained by aggregation of two parthenogenetic morulae without donor ICMs were also transferred to a recipient to verify the developmental ability of the host embryos.

Crossbred (Large White/Landrace × Duroc) prepubertal gilts, weighing between 100 and 105 kg, were used as the recipients of the chimeric blastocysts. The gilts were given a single intramuscular (i.m.) injection of 1,000 IU eCG (ASKA Pharmaceutical) to induce estrus. Ovulation was induced by an i.m. injection of 1,500 IU hCG (Kyoritsu Seiyaku Corporation, Tokyo, Japan), which was given 66 hr after the injection of eCG. The blastocysts were surgically transferred into the uterine horns of the recipients approximately 146 hr after hCG injection.

Evaluation of Chimerism in the Fetuses

The recipient gilts were autopsied on day 18 of gestation to collect somite stage fetuses. Fetuses showing the huKO-fluorescence in fluorescence microscopy (MVX10, Olympus) were evaluated to be chimeric. Chimerism was verified by PCR amplifying the sequences of huKO transgene in the genomic DNA extracted from the fetuses using DNeasy Blood and Tissue Kit (QIAGEN, Inc., Hilden, Germany).

Fetuses were also analyzed by genotyping to detect female/male chimerism. In the present study, chimeric embryos were composed of parthenogenetic host embryos; hence, the sex chromosome composition of those embryos was XX. However, half of the donor ICMs obtained from the IVF blastocysts theoretically had XY-chromosome composition. Therefore, detection of Y chromosome-specific sequences [40] in the fetuses' genomic DNA was used to determine the chimerism. Nested PCR for detection of huKO transgene was performed using following primers: 5′- AGCACGAAGTCTGGAGACCTCTG-3′ and 5′- AGGTGGTCTTGAACTGGCACTTGTG-3′ for the first round of PCR; 5′- ACCTTACACAGTCCTGCAGACC-3′ and 5′- GCCAGCTTCAGGAACATGGT-3′ for the second round of PCR. The cycle conditions of both PCR were 95°C for 1 min, followed by 95°C for 30 sec, 68°C for 30 sec, and 72°C for 1 min per cycle for 25 cycles. The primers used to amplify the porcine male-specific sequences for sex determination were 5′- AAGTGGT-

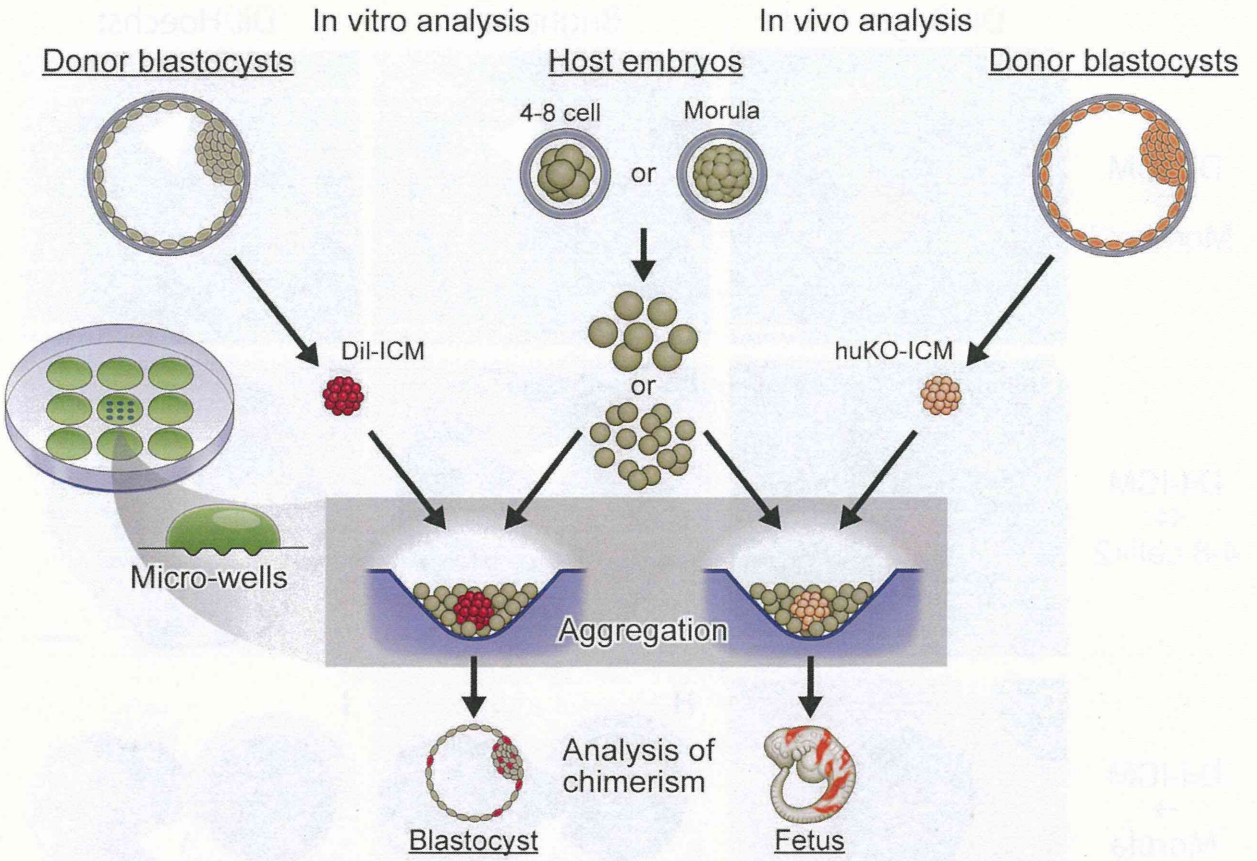

Figure 1. Generalized scheme for the production of chimeric porcine blastocysts and fetuses by the aggregation method. For *in vitro* analysis of the chimeric blastocyst formation, donor ICMs were isolated from parthenogenetic blastocysts derived from IVM oocytes. Isolated ICMs stained with DiI were aggregated with blastomeres isolated from parthenogenetic host embryos in a microwell made on the bottom of a culture dish. For *in vivo* analysis of chimeric fetus formation, the donor ICMs were isolated from blastocysts fertilized *in vitro* by transgenic boar sperm carrying the fluorescent huKO gene. ICMs of the IVF blastocysts were similarly aggregated with the parthenogenetic host embryos as the DiI-stained ICMs, and the resultant blastocysts were transferred to recipient pigs to obtain chimeric fetuses.
doi:10.1371/journal.pone.0061900.g001

CAGCGTGTCCATA-3′ and 5′-TTTCTCCTGTATCCTCCTGC-3′ [40]. The cycle conditions were 95°C for 1 min, followed by 95°C for 30 sec, 58°C for 5 sec, and 72°C for 20 sec per cycle for 25 cycles.

To quantify chimerism of the fetuses, sagittal sections of the huKO-positive fetuses were analyzed after immunostaining with polyclonal antibody against huKO (MBL Co., Ltd., Nagoya, Japan). The chimeric fetuses with fluorescence were fixed with 4% (w/v) paraformaldehyde, embedded in paraffin blocks and thin-sectioned. Paraffin-embedded sections were deparaffinized with xylene and hydrated with graded ethanols. Each section was incubated with anti-huKO antibody (1:100) for 0.5 hr at room temperature. Distribution of huKO expressing cells in each section was determined by peroxidase staining using Histofine® kit (Nichirei Biosciences, Inc., Tokyo, Japan) with haematoxylin counterstaining. Proportion of the huKO-positive cells in the sections covering entire body of the fetuses was measured by image analysis software (ImageJ, http://rsb.info.nih.gov/ij/).

Statistics Analysis

Statistical analyses were performed using the SPSS 16.0 software (SPSS, Inc., Chicago, IL, USA). Differences between two groups were analyzed using the χ^2-test. For comparisons among three groups or more, the data were subjected to arcsine transformation and evaluated by one-way analysis of variance (ANOVA) followed by multiple comparisons by Tukey's test. The level of significance was set at $P<0.05$.

Results and Discussion

Aggregation of Donor ICMs and Parthenogenetic Blastomeres to Produce Chimeric Blastocysts

Our first step was to address the question of whether chimeric blastocysts could be produced efficiently *in vitro* using ICMs as the donor cells for aggregation with parthenogenetic embryos. At the same time, we sought to determine whether the developmental stage of the host embryos influenced the production rate of chimeras (Figure 1).

Intact ICMs isolated from parthenogenetic blastocysts by immunosurgery [22] were used as the donor cells. Each ICM was first stained with DiI and then placed into a microwell [41] with blastomeres disaggregated from two parthenogenetic morulae (Figure 2A). After culture, 95.8% (23/24) of the aggregates developed to form single blastocysts (Figure 2B, Table 1). Fluorescent DiI signals derived from the donor ICMs were observed in 20 of the 23 blastocysts (87.0% or 83.3% of the

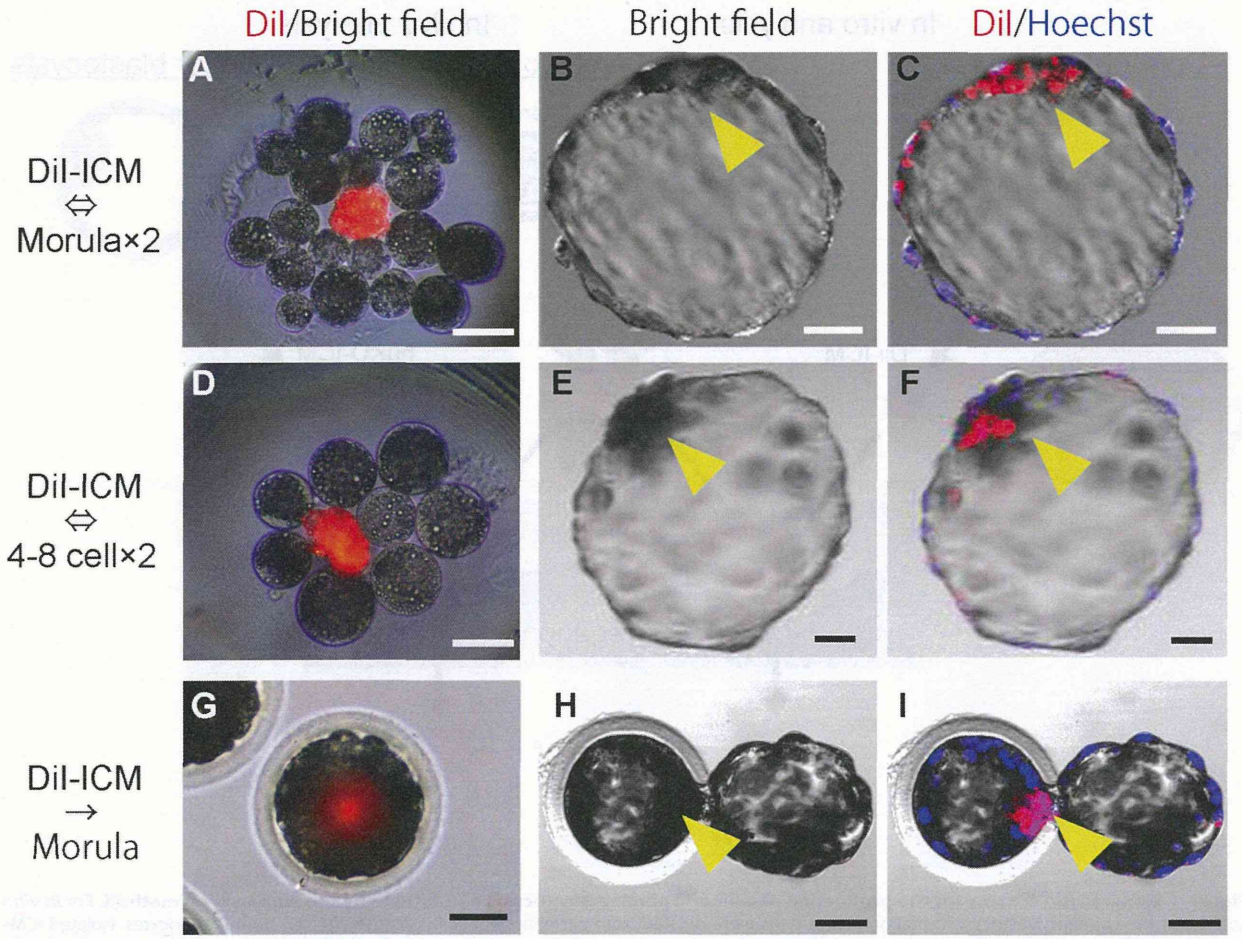

Figure 2. Production of chimeric blastocysts with donor ICM and parthenogenetic host embryos. (A, D) A donor ICM (stained with DiI) aggregated with host blastomeres isolated from parthenogenetic embryos at the morula (A) or 4–8 cell stage (D). (B, E) Bright field images of chimeric blastocysts developed from the aggregated embryos. (C, F) Confocal fluorescence images of chimeric blastocysts showing DiI fluorescence in ICMs. Single confocal sections of fluorescence were overlaid on the bright field images. (G-I) Parthenogenetic host morulae injected with DiI-stained donor ICM (G) and resultant chimeric blastocysts (H, I). Arrow heads, ICM. Scale bars = 50 μm.
doi:10.1371/journal.pone.0061900.g002

embryos cultured) (Figure 2C). Thus, a high rate of formation of chimeric blastocysts was achieved, which was similar to the outcome obtained when donor ICMs were injected into parthenogenetic morulae (Figure 2G–I, Table 1).

We also carried out an aggregation experiment using DiI-stained ICMs and 4–8 cell-stage parthenogenetic embryos (Figure 2D). Blastocysts were formed in 88.5% (23/26) of the aggregates (Figure 2E), and 65.4% (17/26) were chimeric (Figure 2F). The rates of blastocyst and chimera formation were not significantly different from those obtained using morulae.

With these results, we have demonstrated that the efficient production of chimeric blastocysts can be achieved by an aggregation method using donor ICMs and host parthenogenetic embryos. The developmental stage of the host embryo does not appear to be a limiting factor, as equally efficient chimera production occurred with 4–8 cell-stage embryos (day 3), which are more distant in developmental stage from the donor ICMs (day 6), compared to morula stage embryos (day 4). We believe that the ability of the aggregation method to use a wider range of host embryonic stages has practical significance.

We also confirmed that the efficiency of chimeric blastocyst production by the aggregation method using donor ICMs and host blastomeres was similar to that using aggregation of host and donor blastomeres (Table 1). The formation rates of chimeric blastocysts using ICMs (Figure 2A–C) or morula-blastomeres (Figure 3A–C) as the donor cells with morula stage host embryos were 83.3% (20/24) and 70.6% (24/34), respectively (not significantly different). Similarly, when 4–8 cell-stage embryos were used as the host, donor ICMs (Figure 2D–F) produced 65.4% (17/26) chimeric blastocysts compared to 58.7% (27/46) using synchronous (4–8 cell stage, Figure 3D–F) donor blastomeres and 65.4% (17/26) using asynchronous (morula stage, Figure 3G–I) donor blastomeres (not significantly different in either case).

In the present study, the donor ICMs were not disaggregated into single cells, but this did not appear to inhibit their incorporation by the host embryos. This suggests that iPS cells that form cellular colonies during development should also be able to aggregate with host blastomeres. However, in porcine iPS colonies with naïve type morphological characteristics, we found partially differentiated cell fractions in which *Oct3/4* promoters are highly methylated [12]. We also recently found that porcine iPS

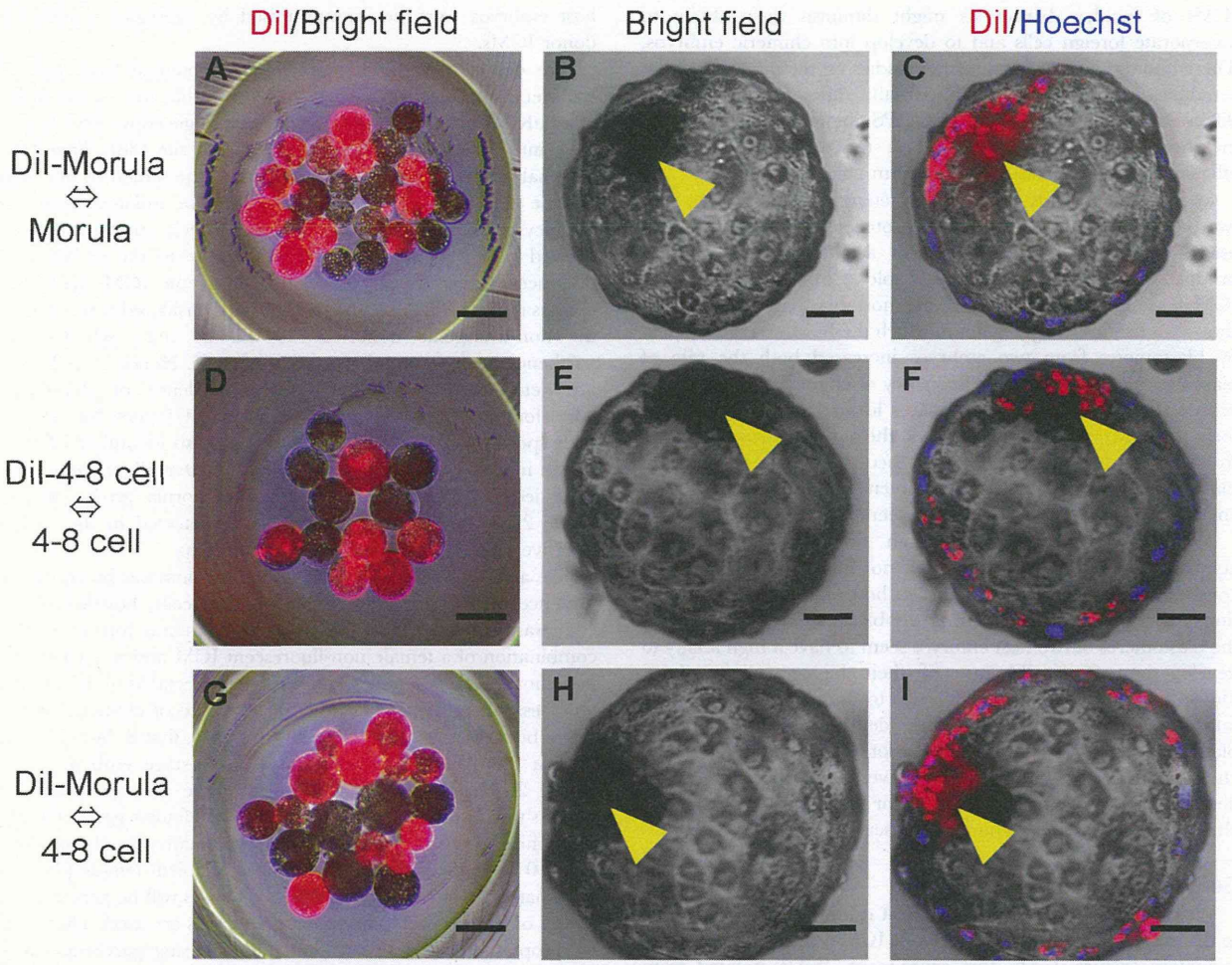

Figure 3. Production of chimeric blastocysts by blastomere aggregation. (A, D, G) Aggregation of donor (DiI-stained) and host blastomeres between synchronous (A, D) and asynchronous (G) embryonic stages. (B, E, H) Chimeric blastocysts developed from the aggregated blastomeres. (C, F, I) Confocal fluorescence images of the chimeric blastocysts showing DiI fluorescence in ICMs. Single confocal sections of fluorescence were overlaid on the bright field images. Arrow heads, ICM. Scale bars = 50 μm.
doi:10.1371/journal.pone.0061900.g003

colonies with epistem cell (primed)-like characters show a reduced rate of chimeric blastocyst formation after aggregation with blastomeres (unpublished). Furthermore, Tachibana *et al.* reported that monkey blastocysts did not readily aggregate with transplanted ICMs to form chimeric embryos [42]. They identified two types of cells within monkey ICMs: a cluster of NANOG-positive epiblast cells and a covering layer of GATA-6-positive primitive endoderm cells. They suggested that cellular segregation in the

Table 1. *In vitro* development of the chimeric embryos produced by injection or aggregation method.

Donor cells	Method	Stage of host embryos	No. of embryos cultured	Blastocysts (%)	Chimeric blastocysts (%)
ICM	Injection	Mourla	29	27 (93.1)	24 (82.8)
ICM	Aggregation	Morula**	24	23 (95.8)	20 (83.3)
ICM		4–8 cell**	26	23 (88.5)	17 (65.4)
Morula*		Morula*	34	31 (91.2)	24 (70.6)
Morula*		4–8 cell*	26	23 (88.5)	17 (65.4)
4–8 cell*		4–8 cell*	46	37 (80.4)	27 (58.7)

*Blastomeres isolated from single embryos.
**Blastomeres isolated from two embryos.
doi:10.1371/journal.pone.0061900.t001

ICMs of monkey blastocysts might diminish their ability to incorporate foreign cells and to develop into chimeric embryos. These findings indicate that further studies on the influence of the simultaneous presence of both partially differentiated and undifferentiated pluripotent cells in an iPS colony are necessary for investigating any possible effects on the ability to aggregate efficiently with host blastomeres to form chimeras.

In the present study, we routinely cultured donor ICMs with two parthenogenetic embryos. This protocol was adopted because use of a single morula resulted in a relatively low rate of production of chimeric blastocysts (Table 1); in many cultures, the ICM was not incorporated by the host blastomeres (data not shown). By contrast, aggregates in which the ICM was sandwiched by blastomeres from two embryos increased both the rate of blastocyst formation and the frequency of chimerism. It has been proposed previously that blastomeres located inside the morula form the ICM, while those located on the outside differentiate into trophectoderm (the "inside-outside" theory [43]). We suggest that sandwiching the donor ICM between blastomeres from two embryos is the cause of the high frequency of ICM chimerism.

As parthenogenetic embryos can be obtained easily by activating IVM oocytes, there is no increased difficulty in conducting the experiment using two host embryos per aggregation. An additional benefit is that the blastocysts generated from the blastomeres of two host embryos seem to have a high ability to develop into fetuses because of their higher cell numbers. However, the ratio of donor cells to host blastomeres may influence the rate of aggregates developing into chimeric blastocysts as well as the contribution of the donor cells to chimeric fetuses [44,45]. Further investigation is required to determine the optimal conditions for efficient production of chimeric blastocysts and chimeric fetuses.

Generation of Chimeric Fetuses

We carried out a transfer experiment using chimeric blastocysts to determine the contribution of donor ICM cells to chimeric fetus formation (Figure 1). In this experiment, ICMs isolated from transgenic blastocysts carrying the huKO gene were aggregated with blastomeres of parthenogenetic morulae or 4–8 cell-stage embryos. We produced 102 and 67 aggregated embryos using host embryos at the morula and 4–8 cell stages, respectively (Table 2). In total, 73 (71.6%) and 54 (80.6%) blastocysts (Figure 4A, B), respectively, developed to blastocysts and were transferred into 2 recipient gilts; all gilts were successfully impregnated.

On day 18 of gestation, the gilts were subjected to laparotomy. In total, 25 (34.2%) fetuses were recovered from the "morula" group, while 22 (40.7%) were recovered from the "4–8 cell-stage embryo" group; the difference in the developmental rate between the groups was not significant (Table 2). A PCR analysis to detect the huKO transgene showed that 6/25 (24.0%) and 3/22 (13.6%) fetuses were chimeric (Table 2). All the PCR-positive fetuses were fluorescent due to expression of huKO, although the intensity of fluorescence varied among the fetuses indicating the presence of variation in the proportion of donor ICM derived cells among the chimeric fetuses (Figure 4). An immunostaining analysis of 6 huKO-positive fetuses showed that the proportion of donor cells in the chimeras ranged from 16 to 65% (Figure 4E, H, K). The donor cells were distributed throughout the whole body of the fetuses with no indication of any localization of huKO cells to specific organs or tissues (data not shown).

When 20 of the blastocysts developed from aggregates of two parthenogenetic morulae were transferred to a recipient, 5 (25.0%) developed to somite-stage fetuses (day 22, Figure 4O–Q), suggesting that developmental competence of the parthenogenetic host embryos were not compromised by aggregation with the donor ICMs.

The donor ICMs in this study were obtained from huKO-transgenic blastocysts produced by *in vitro* fertilization using semen of a huKO-transgenic boar that carried a single copy of the huKO gene integrated into a single chromosomal site [38]. Therefore, only half of the blastocysts obtained using the semen of this boar will be transgenic [37]. When ICMs were isolated from the blastocysts, we did not carry out any check on whether they showed huKO expression to avoid damage to the embryos by fluorescence microscopy. Thus, non-transgenic ICMs had been used as donor cells. A second factor to be considered is that half of the non-transgenic donor ICMs will be male whereas the parthenogenetic host embryos are all female. Hence, if male cells are detected in the fetuses, this is evidence of chimerism. Therefore, we screened the non-fluorescent fetuses for porcine male specific DNA sequence [40]; this analysis identified 3 fetuses in the morula group that were chimeras. Overall, therefore, we identified 9/25 chimeric fetuses in the morula group (36.0%, Table 2). No male-specific signals were detected in the huKO negative fetuses in the 4–8 cell embryo group.

The analyses described above identified chimeras based on the presence of the huKO transgene or male cells; however, other chimeras may also exist. For example, chimeras formed by the combination of a female non-fluorescent ICM and a parthenogenetic host embryo (female) would not be detectable in the present analyses. Therefore, we believe that the rate of chimeric fetuses might be greater than the detected frequency, that is, 36.0% in the morula group and 13.6% in the 4–8 cell-stage embryo group (Table 2). Regardless, we have shown here that our approach ensures that at least one fetus out of every 10 fetuses generated will be a chimera. As it is a relatively simple matter to obtain more than 10 parthenogenetic fetuses from a recipient female [32], we anticipate that one to several chimeric fetuses will be generated in a litter of fetuses when pluripotent donor cells are used. Therefore, we propose that the aggregation method using parthenogenetic host embryos is a practical approach to the evaluation of the pluripotency of iPS cells.

The aggregation method using host parthenogenetic embryos is straightforward; however, parthenogenetic embryos are expected to be restricted in their developmental capacity to the somite stage and are not expected to produce liveborn young [31,32,46]. In the present study, we sought to establish a method for evaluating the comparative ability of donor cells to contribute to chimeric fetuses and were not interested in the production of chimeric offspring. However, even somite stage fetuses can be valuable for tracking the differentiation of endoderm, mesoderm, and ectoderm tissues [33]. Gonadal specification can also be examined. When chimeric fetuses after the somite stage or liveborn offspring are required, it will be necessary to use IVF embryos or *in vivo*-derived embryos to provide the host cells for the aggregation method.

Conclusion

We have demonstrated that chimeric fetuses can be produced in a highly reproducible manner by aggregation of host parthenogenetic embryos at the morula or 4–8 cell stages with donor ICM cells. To the best of our knowledge, this is the first demonstration that aggregation with parthenogenetic blastomeres is an effective means of determining pluripotency in porcine cells. The method provides a simple and highly accurate system for evaluating whether undifferentiated cells such as iPS cells possess the chimera formation ability characteristic of true pluripotency.

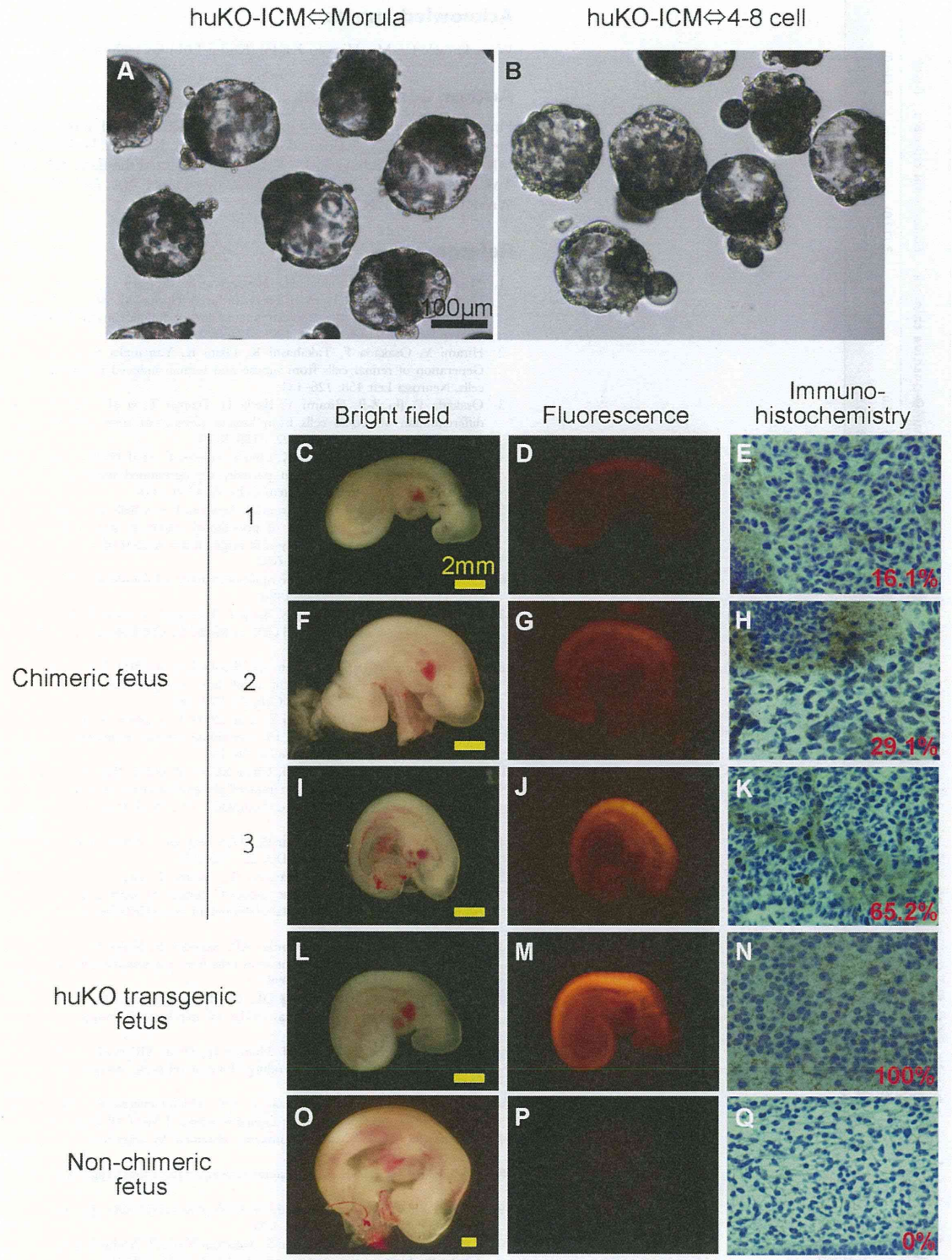

Figure 4. Chimeric fetuses produced by aggregation of the ICM carrying huKO transgene and parthenogenetic host embryos. (A, B) Morphological appearance of the chimeric blastocysts before embryo transfer. (C–K) Chimeric fetuses (day 18) showing huKO fluorescence derived from the donor ICM cells (C, D, F, G, I, J) and immunohistochemical images showing proportion of the donor-derived (huKO-positive) cells in the tissue of chimeric fetuses (E, H, K). (L, M, N) A day-19 fetus developed from an embryo fertilized *in vitro* with the huKO transgenic boar sperm as a positive control, showing the systemic expression of huKO (M, N). (O, P, Q) A non-chimeric fetus (day 22) developed from the aggregates of two parthenogenetic embryos as a negative control.
doi:10.1371/journal.pone.0061900.g004

Table 2. Development of the aggregated embryos into chimeric fetuses.

Stage of host embryos	Aggregated embryos produced	Developed to blastocysts (%)	Blastocysts transferred	Pregnancy	Developed to fetuses (%)	Chimeric fetuses (%)		
						huKO-positive chimera	Male-femal chimera	Total
Morula	102	73 (71.6)	73	2/2	25 (34.2)	6 (24.0)	3 (12.0)	9 (36.0)
4–8 cell	67	54 (80.6)	54	2/2	22 (40.7)	3 (13.6)	0 (0)	3 (13.6)

doi:10.1371/journal.pone.0061900.t002

Acknowledgments

We acknowledge Mr. Hiroshi Kadoi (Kadoi Ltd.) for technical help.

Author Contributions

Final approval of the manuscript: MN YH HN. Conceived and designed the experiments: HN. Performed the experiments: KN MW HM TM KH MM TK GH M. Kobayashi M. Kuramoto. Analyzed the data: KN MW TM. Contributed reagents/materials/analysis tools: YA KU SF YM. Wrote the paper: KN MW MN HN.

References

1. Miki K, Saito A, Uenaka H, Miyagawa S, Shimizu T, et al. (2009) Cardiomyocyte Sheets Derived From Induced Pluripotent Stem (iPS) Cells Improve Cardiac Function and Attenuate Cardiac Remodeling in Myocardial Infarction in Mice. Circulation 120: S721–S721.
2. Hirami Y, Osakada F, Takahashi K, Okita K, Yamanaka S, et al. (2009) Generation of retinal cells from mouse and human induced pluripotent stem cells. Neurosci Lett 458: 126–131.
3. Osakada F, Jin Z-B, Hirami Y, Ikeda H, Danjyo T, et al. (2009) In vitro differentiation of retinal cells from human pluripotent stem cells by small-molecule induction. J Cell Sci 122: 3169–3179.
4. Matsui T, Takano M, Yoshida K, Ono S, Fujisaki C, et al. (2012) Neural stem cells directly differentiated from partially reprogrammed fibroblasts rapidly acquire gliogenic competency. Stem Cells 30: 1109–1119.
5. van der Spoel TI, Jansen of Lorkeers SJ, Agostoni P, van Belle E, Gyongyosi M, et al. (2011) Human relevance of pre-clinical studies in stem cell therapy: systematic review and meta-analysis of large animal models of ischaemic heart disease. Cardiovasc Res 91: 649–658.
6. Zhao MT, Prather RS (2011) The multi-potentiality of skin-derived stem cells in pigs. Theriogenology 75: 1372–1380.
7. Montserrat N, Garreta Bahima E, Batlle L, Haefner S, Cavaco Rodrigues AM, et al. (2011) Generation of Pig iPS Cells: A Model for Cell Therapy. J Cardiovasc Transl Res 4: 121–130.
8. Zhou L, Wang W, Liu Y, de Castro JF, Ezashi T, et al. (2011) Differentiation of induced pluripotent stem cells of swine into rod photoreceptors and their integration into the retina. Stem Cells 29: 972–980.
9. Li W, Wei W, Zhu S, Zhu J, Shi Y, et al. (2009) Generation of rat and human induced pluripotent stem cells by combining genetic reprogramming and chemical inhibitors. Cell Stem Cell 4: 16–19.
10. Wang W, Yang J, Liu H, Lu D, Chen XF, et al. (2011) Rapid and efficient reprogramming of somatic cells to induced pluripotent stem cells by retinoic acid receptor gamma and liver receptor homolog 1. Proc Natl Acad Sci U S A 108: 18283–18288.
11. De Los Angeles A, Loh YH, Tesar PJ, Daley GQ (2012) Accessing naïve human pluripotency. Curr Opin Genet Dev 22: 272–282.
12. Fujishiro SH, Nakano K, Mizukami Y, Azami T, Arai Y, et al. (2012) Generation of naive-like porcine induced pluripotent stem cells capable of contributing to embryonic and fetal development. Stem Cells Dev; DOI101089/scd20120173.
13. Ezashi T, Telugu BPVL, Alexenko AP, Sachdev S, Sinha S, et al. (2009) Derivation of induced pluripotent stem cells from pig somatic cells. Proc Natl Acad Sci U S A 106: 10993–10998.
14. Esteban MA, Peng MX, Zhang DL, Cai J, Yang JY, et al. (2010) Porcine induced pluripotent stem cells may bridge the gap between mouse and human iPS. IUBMB Life 62: 277–282.
15. West FD, Terlouw SL, Kwon DJ, Mumaw JL, Dhara SK, et al. (2010) Porcine induced pluripotent stem cells produce chimeric offspring. Stem Cells Dev 19: 1211–1220.
16. Wu Z, Chen J, Ren J, Bao L, Liao J, et al. (2010) Generation of pig-induced pluripotent stem cells with a drug-inducible system. J Mol Cell Biol 2: 104–104.
17. Gardner RL (1968) Mouse chimaeras obtained by injection of cells into blastocyst. Nature 220: 596–597.
18. Tarkowski A (1961) Mouse chimaeras developed from fused eggs. Nature 190: 857–860.
19. Mintz B (1962) Experimental study or developing mammalian egg - removal of zona pellucida. Science 138: 594–595.
20. Kashiwazaki N, Nakao H, Ohtani S, Nakatsuji N (1992) Production of chimeric pigs by the blastocyst injection method. Vet Rec 130: 186–187.
21. Mueller S, Prelle K, Rieger N, Petznek H, Lassnig C, et al. (1999) Chimeric pigs following blastocyst injection of transgenic porcine primordial germ cells. Mol Reprod Dev 54: 244–254.
22. Nagashima H, Giannakis C, Ashman R, Nottle M (2004) Sex differentiation and germ cell production in chimeric pigs produced by inner cell mass injection into blastocysts. Biol Reprod 70: 702–707.
23. Onishi A, Takeda K, Komatsu M, Akita T, Kojima T (1994) Production of chimeric pigs and the analysis of chimerism using mitochondrial deoxyribonucleic-acid as a cell marker. Biol Reprod 51: 1069–1075.

24. Piedrahita JA, Moore K, Oetama B, Lee CK, Scales N, et al. (1998) Generation of transgenic porcine chimeras using primordial germ cell-derived colonies. Biol Reprod 58: 1321–1329.
25. Prather RS, Hoffman KE, Schoenbeck RA, Stumpf TT, Li J (1996) Characterization of DNA synthesis during the 2-cell stage and the production of tetraploid chimeric pig embryos. Mol Reprod Dev 45: 38–42.
26. Shim H, Gutierrez-Adan A, Chen LR, BonDurant RH, Behboodi E, et al. (1997) Isolation of pluripotent stem cells from cultured porcine primordial germ cells. Biol Reprod 57: 1089–1095.
27. Eakin G, Hadjantonakis A (2006) Production of chimeras by aggregation of embryonic stem cells with diploid or tetraploid mouse embryos. Nat Protoc 1: 1145–1153.
28. Abeydeera LR (2002) In vitro production of embryos in swine. Theriogenology 57: 257–273.
29. Gajda B (2009) Factors and methods of pig oocyte and embryo quality improvement and their application in reproductive biotechnology. Reprod Biol 9: 97–112.
30. Dang-Nguyen TQ, Somfai T, Haraguchi S, Kikuchi K, Tajima A, et al. (2011) In vitro production of porcine embryos: current status, future perspectives and alternative applications. Anim Sci J 82: 374–382.
31. Kure-Bayashi S, Miyake M, Okada K, Kato S (2000) Successful implantation of in vitro-matured, electro-activated oocytes in the pig. Theriogenology 53: 1105–1119.
32. Kurihara T, Kurome M, Wako N, Ochiai T, Mizuno K, et al. (2002) Developmental competence of in vitro matured porcine oocytes after electrical activation. J Reprod Dev 48: 271–279.
33. Ogawa B, Ueno S, Nakayama N, Matsunari H, Nakano K, et al. (2010) Developmental ability of porcine in vitro matured oocytes at the meiosis II stage after vitrification. J Reprod Dev 56: 356–361.
34. Matsunari H, Maehara M, Nakano K, Ikezawa Y, Hagiwara Y, et al. (2012) Hollow Fiber Vitrification: a novel method for vitrifying multiple embryos in a single device. J Reprod Dev 58: 599–608.
35. Petters R, Wells K (1993) Culture of pig embryos. J Reprod Fertil Suppl 48: 61–73.
36. Funahashi H, Day B (1993) Effects of the duration of exposure to hormone supplements on cytoplasmic maturation of pig oocytes in vitro. J Reprod Fertil 98: 179–185.
37. Maehara M, Matsunari H, Honda K, Nakano K, Takeuchi Y, et al. (2012) Hollow fiber vitrification provides a novel method for cryopreserving in vitro maturation/fertilization-derived porcine embryos. Biol Reprod; DOI101095/biolreprod112100339.
38. Kanai T, matsunari H, Takeuchi Y, Honda K, Maehara M, et al. (2012) Transmission and expression of a retrovirally introduced red fluorescent protein gene in successive generations of transgenic pigs. Reprod Domest Anim 47: 605.
39. Yoshioka K, Suzuki C, Onishi A (2008) Defined system for in vitro production of porcine embryos using a single basic medium. J Reprod Dev 54: 208–213.
40. Kawarasaki T, Kohsaka T, Sone M, Yoshida M, Bamba K (1995) Detection of Y-bearing porcine spermatozoa by in-situ hybridization usin digoxigenin-labeled, porcine male-specific dna-probe produced by polymerase chain-reaction. Mol Reprod Dev 40: 455–459.
41. Nagy A, Rossant J (1993) Production of completely ES cell-derived fetuses. In: Joyner A, editor. Gene Targeting: A Practical Approach. Oxford University Press.
42. Tachibana M, Sparman M, Ramsey C, Ma H, Lee H-S, et al. (2012) Generation of chimeric rhesus monkeys. Cell 148: 285–295.
43. Tarkowsk.Ak Wroblews.J (1967) Development of blastomeres of mouse eggs isolated at 4- and 8-cell stage. J Embryol Exp Morphol 18: 155–180.
44. Hillman N, Sherman MI, Graham C (1972) Effect of spatial arrangement on cell determination during mouse development. J Embryol Exp Morphol 28: 263–278.
45. Tsuji H, Kuriyama K (1990) Development of rat-mouse interspecific embryos in pseudopregnant rat uterus. Jpn J Zootech Sci 61: 913–918.
46. Zhu J, King T, Dobrinsky J, Harkness L, Ferrier T, et al. (2003) In vitro and in vivo developmental competence of ovulated and in vitro matured porcine oocytes activated by electrical activation. Cloning Stem Cells 5: 355–365.

第74回日本血液学会学術集会
Presidential Symposium
Innovative Gene & Cell Therapy for Hematological Diseases

大型動物を用いた幹細胞研究

花園 豊

Key words : Stem cells, Monkeys, Sheep, Pigs

1. はじめに

エドワード・ドナル・トーマス博士は，昨年（2012年）亡くなった（享年92歳）。1958年骨髄移植を世界で初めて実施し，その功績で1990年ノーベル医学生理学賞を受賞した。しかし，トーマス博士が始めた骨髄移植が世に認められるまでの道のりは決して平坦ではなかった。ライナー・ストーブ博士の弔辞の中で言及されている通り，1970年代まで骨髄移植が成功すると信じる人は少なかったという[1]。しかし今や，この治療はさまざまな血液・悪性疾患や先天性疾患の根治療法として確立し広く普及している。そればかりでなく，より多くの患者に対していっそう安全・低負担かつ効果的に実施できるように，現在も日夜，精力的に研究が進められている。骨髄移植の成功と発展を見て一番喜んだのはトーマス博士その人だったのではなかろうか。

骨髄移植に始まる造血幹細胞移植の研究は，造血幹細胞の効率的な単離・増幅・遺伝子導入法や，患者への前処置・移植・支持療法の改良・開発など多岐にわたる。造血幹細胞のソースとして，現在，骨髄・末梢血・臍帯血が使用されているが，人工多能性幹細胞（iPS細胞）をソースとして利用する研究も始まった[2]。その多くは，まず，マウスの系で結果が示される。しかし，マウス実験からヒト臨床へひとっ飛びではいかない。造血幹細胞の移植治療において有効性と安全性の担保が常に必要とされる。それにはマウスのような小型動物を用いた評価系は必要だが必ずしも十分ではない。

特に安全性評価に関しては，過去の歴史が如実に実証している。ヒト造血幹細胞遺伝子治療で，レトロウイルスベクターに起因する挿入変異発癌が2000年以降相次いで報告されて話題になったが[3,4]，これらの有害事象はマウス実験では検出されていなかった点が問題である。これには幾つかの理由があろう。一つには，マウスのような短命・小型動物ゆえの時空間的なスケールの問題があると考えている[5]。

したがって，新しい血液再生治療の有効性や安全性の評価には大型動物を用いる実験が必要であり，我々は，サルやヒツジやブタを用いて実験している。本総説ではその成果をレビューしたい。

2. リンパ球遺伝子治療と造血幹細胞遺伝子治療

筆者は，1995年から米国立衛生研究所（NIH）に滞在して初めてサルを用いた研究を始めた。当時のアメリカはクリントン大統領の施政下，莫大な政府予算を遺伝子治療研究につぎ込み，世界中から研究者を引き付けていた。私もその一人だった。この頃，マウスの好データを頼りに始まったヒトの遺伝子治療の失敗が続き，筆者が渡米した1995年はNIHからOrkin-Motulskyの勧告が出された年だった。それは，「臨床研究を急がず基礎研究を着実に進めること，臨床応用の前にサルなど大型動物で検証実験を実施するように」という内容だった。この勧告に基づいてNIHはサル研究に莫大な予算を投入するようになった。こうして，元々マウスで開発された遺伝子治療技術がヒト向けに改良されていった。筆者もサルを使って研究を進め，面白いことにヒト向けの遺伝子治療プロトコールは，マウス向けのものとは全く異なったものが出来上がってくることに気づいた[6]。それからおよそ10年経ち造血幹細胞遺伝子治療もようやく成功例が出て来た[7~9]。とはいえ，レトロウイルスベクターの実用にはまだ解決すべき課題が多く残っている[10]。トーマス博士に始まった骨髄移植と同様の歴史（失敗と失望の後の成功と普及）がここでも繰り返され

自治医科大学 分子病態治療研究センター 再生医学研究部

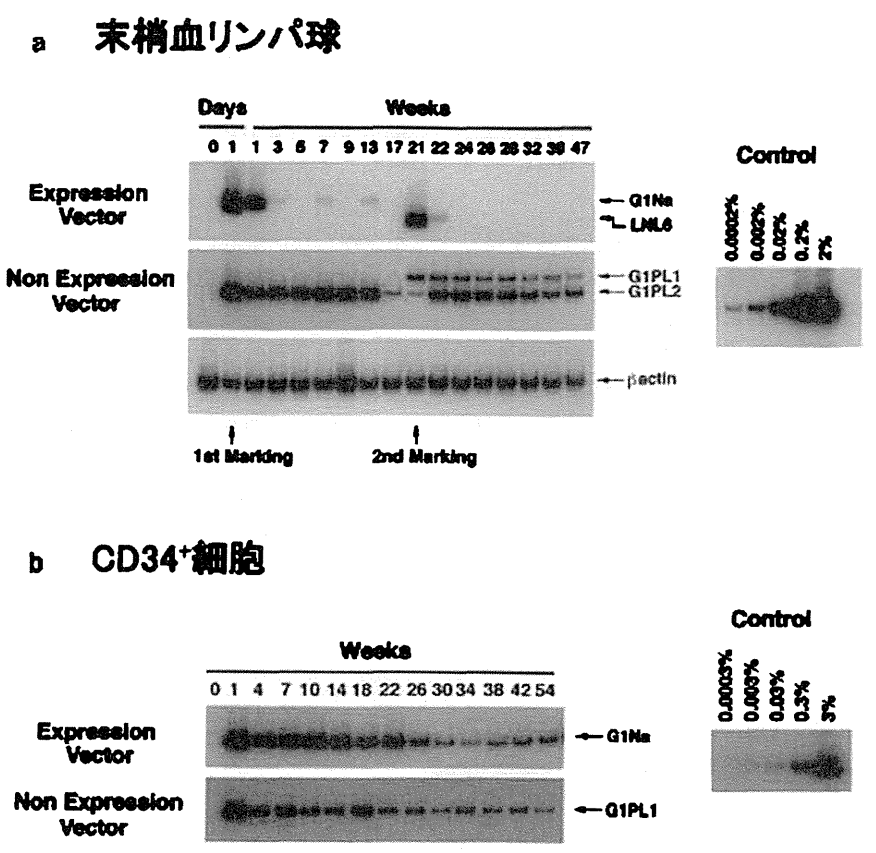

図 1　リンパ球遺伝子治療と造血幹細胞遺伝子治療
サルを用いた実験。(a) レトロウイルスベクター（G1Na と LNL6）で外来遺伝子（ここではネオマイシン耐性遺伝子 *neo*）を導入したリンパ球は自家輸注しても直ちに排除される。一方，空のレトロウイス（G1PL1 と G1PLII）を感染させたリンパ球は排除されない。(b) 同じ遺伝子（*neo*）を造血幹細胞に導入してから移植すると，遺伝子導入細胞は排除されない。造血幹細胞に導入した遺伝子に対しては免疫寛容が誘導される。

るのであろうか。

私が NIH で実施した研究を一つ紹介したい（図 1）[11]。サルから末梢リンパ球または造血幹細胞（$CD34^+$ 細胞）を採取して均等な二群に分ける。それぞれの群をネオマイシン耐性遺伝子（*neo*）を発現するレトロウイルスまたは何も発現しないレトロウイルスで感染させる。両群を元のサルに輸注（自家移植）する。輸注後，両群の運命を調べた。リンパ球を標的とした場合，*neo* 導入リンパ球は，早くも輸注 3 週後には消失してしまった。一方，対照として空ベクターを導入したリンパ球は輸注後 1 年以上にわたって安定的に末梢血中に検出された。すなわち，リンパ球に外来遺伝子を導入して体内に戻せば免疫排除されてしまう。リンパ球遺伝子治療については再検討が必要と考えられた。

他方，造血幹細胞を標的にすると，全く異なる結果が得られた。すなわち，*neo* を導入したリンパ球も，空ベクターを導入したリンパ球も，いずれの群も輸注後 1 年以上にわたって安定的に末梢血中に検出された。造血幹細胞を標的とする遺伝子治療なら，外来遺伝子を導入しても排除されず（おそらく免疫寛容が誘導される），遺伝子治療として成立し得る。しかし，大きな課題も残った。造血幹細胞を標的とする場合，末梢血の 1%程度にしか遺伝子を導入できず，遺伝子導入効率が極端に低かったのである。これも我々のサル実験から初めて判明したことで，マウス実験からは予測できなかったことである。

3. 造血幹細胞遺伝子治療における増殖優位性の重要性

帰国後，造血幹細胞遺伝子治療の実現をめざして，霊長類医科学研究センター（筑波）と共同でサルを用いた実験を続けた。このことについて以前本誌に総説を上梓